

# **Mechanisms of stability of rhodolith beds: sedimentological aspects**

by

Kyle R. Millar

©

A thesis submitted to the  
School of Graduate Studies  
in partial fulfillment of the  
requirements for the degree of  
Master of Science

Department of Ocean Sciences

Memorial University of Newfoundland

December, 2017

St. John's, Newfoundland, Canada

## ABSTRACT

Rhodolith beds are highly diverse benthic communities organized around the physical structure and primary productivity of red coralline algae. Despite a worldwide distribution and growing recognition that rhodolith beds are important calcium carbonate ( $\text{CaCO}_3$ ) bio-factories, little is known of the factors and processes that regulate their structure, function, and stability. One prevalent and largely untested paradigm is that beds develop in environments where water motion is strong enough to prevent burial by sediments. Observations over seven months and three weeks in the centre and near the upper and lower margins of a Newfoundland rhodolith (*Lithothamnion glaciale*) bed, as well as a laboratory mesocosm experiment with rhodoliths and dominant macrofauna from the bed, were used to characterize, parse, and model spatial and temporal variation in rhodolith sediment load (RSL) and movement among presumably important abiotic and biotic factors. RSL and movement were largely mediated by a few dominant benthic invertebrates. Hydrodynamic forces were insufficient to displace rhodoliths. Daisy brittle stars (*Ophiopholis aculeata*) and small common sea stars (*Asterias rubens*) contributed to dislodgement of sediment from rhodoliths. Large green sea urchins (*Strongylocentrotus droebachiensis*) easily displaced rhodoliths in mesocosms. Results provide the first quantitative demonstration that rhodolith beds need not be exposed to threshold hydrodynamic conditions to avoid burial. Beds can simply occur in areas where burial is unlikely because of low sedimentation rates. In such cases, select resident bioturbators operating simultaneously at different spatial scales (within and outside rhodoliths) appear to suffice to maintain RSL below lethal quantities, contributing to stability of beds.

## ACKNOWLEDGEMENTS

I thank my supervisor Dr. Patrick Gagnon for his support and encouragement throughout every stage of this project, as well as the other members of my supervisory committee, Dr. Evan Edinger and Dr. Dominique Robert for support and constructive comments that helped improve the thesis. Special thanks to the members of the Gagnon lab for their advice, hard work, and dedication: David Bélanger, Anne Provencher St-Pierre, and Samantha Trueman, as well as to the laboratory research assistants Christa Sandall, Victoria Battcock, and Jadson Lima. I'd like to thank Dr. David Schneider for statistical advice, and Heather Penney for mapping help in R and all-around support. I am also grateful for the support and encouragement of my family and friends. This research was funded by Natural Sciences and Engineering Research Council of Canada (NSERC Discovery Grant), Canada Foundation for Innovation (CFI Leaders Opportunity Funds), and Research & Development Corporation of Newfoundland and Labrador (IngniteR&D) grants to Patrick Gagnon. Kyle Millar was supported by the NSERC Alexander Graham Bell Canada Graduate Scholarship (Master's) program.

## TABLE OF CONTENTS

<b>ABSTRACT</b> .....	ii
<b>ACKNOWLEDGEMENTS</b> .....	iii
<b>TABLE OF CONTENTS</b> .....	iv
<b>LIST OF TABLES</b> .....	vi
<b>LIST OF FIGURES</b> .....	vii
<b>LIST OF APPENDICES</b> .....	x
<b>CO-AUTHORSHIP STATEMENT</b> .....	xi
<b>Chapter I    General Introduction</b> .....	1
<b>Chapter II    Influence of hydrodynamic environment and bioturbation on sediment accumulation in a Newfoundland rhodolith bed</b> .....	9
2.1 INTRODUCTION.....	10
2.2 MATERIALS AND METHODS .....	13
2.2.1 Study site .....	13
2.2.2 Rhodolith sediment load (Field survey 1) .....	14
2.2.3 Rhodolith movement in the field (Field survey 2).....	22
2.2.4 Rhodolith movement by dominant macrofauna (Mesocosm experiment).....	25
2.2.5 Statistical analysis.....	27
2.3 RESULTS .....	33
2.3.1 Field survey 1 .....	33
2.3.2 Field survey 2 .....	43
2.3.3 Mesocosm experiment .....	43
2.4 DISCUSSION.....	49

<b>Chapter III Summary</b> .....	58
3.1. Overall objective of the study.....	59
3.2. Importance of the hydrodynamic environment and bioturbation .....	60
3.3. Importance of the study .....	61
3.4. Future directions .....	62
<b>LITERATURE CITED</b> .....	65
<b>Appendix A</b> .....	74
<b>Appendix B</b> .....	77
<b>Appendix C</b> .....	78
<b>Appendix D</b> .....	83
<b>Appendix E</b> .....	84

## LIST OF TABLES

	Page
<b>Table 2.1</b>	42
Summary of multiple linear regression analysis (applied to raw data) examining the effect of the eight variables included in the best fitting-model of rhodolith sediment load in Field survey 1. DSU = density of large green sea urchins on rhodoliths; DSS = density of large common sea stars on rhodoliths; BBS = biomass (wet weight) of daisy brittle stars within rhodoliths interstices; BRC = biomass of mottled red chitons within rhodoliths interstices; BSU = biomass of small green sea urchins within rhodoliths interstices; BSS = biomass of small common sea stars within rhodoliths interstices; S = sampling station (shallow [12 m] or deep [20 m]); M = sampling month (June to December, 2014) (n=1461).	
<b>Table 2.2</b>	44
Summary of two-way ANOVA (generalized linear model with negative binomial distribution) examining the effect of Depth (12, 16, and 20 m) and Run (three surveys: 1 = mid-November, 2 = late November, and 3 = early December) on movement of marked rhodoliths in Field survey 2 (see section 2.2.3 for a description of the survey).	
<b>Table 2.3</b>	46
Mean water flow speed (WFS), peak WFS, and significant flow speed (SFS) at the shallow (12 m) sampling station during the three late fall surveys in Field survey 2. Water flow velocity was recorded with a Doppler current meter at 5 cm above the rhodolith bed at a rate of 64 readings min <sup>-1</sup> during the first 15 min of every hour. Each data point is the average of the 960 readings in the in the x-, y-, and z-direction available for each hour (see section 2.2.2.1 for details about averaging of flow velocities into dimensionless flow speeds). Mean WFS is the average of all the hourly speed values, whereas SFS is the average of the highest 1/3 of the speed values.	

## LIST OF FIGURES

	Page
<b>Figure 2.1</b>	15
Maps of (A) Newfoundland [eastern Canada] and (B) eastern Conception Bay showing the location of the studied rhodolith bed [diamond] off St. Philip's. (C) Transition [5 m across] between urchin [ <i>Strongylocentrotus droebachiensis</i> ] barrens [upper half] and rhodolith [ <i>Lithothamnion glaciale</i> ] bed [lower half] at a depth of ~10 m [Photo: David Bélanger]. (D) Size [centimeter scale] and shape [primarily spheroidal] of representative rhodoliths from the bed [Photo: Patrick Gagnon].	
<b>Figure 2.2</b>	28
Experimental set-up used to quantify rhodolith movement by green sea urchins ( <i>Strongylocentrotus droebachiensis</i> ) and common sea stars ( <i>Asterias rubens</i> ) (Mesocosm experiment). (A) Location of the nine rhodoliths on the sediment layer covering the experimental area [35 x 30 cm] prior to adding one urchin and one sea star in a trial with both organisms. (B) Location of the rhodoliths, urchin, and sea star at the end [t=4 h] of the same trial. Rhodoliths were marked at the top (white speckles) to facilitate tracking. The white spots in respectively the middle and top of panels A and B are glare from the camera flash used to photograph the experimental area.	
<b>Figure 2.3</b>	34
Mean (+SE) (A) rhodolith sediment load (dry weight) and (B) sedimentation rate (dry weight) at the shallow (12 m) and deep (20 m) stations in the seven months (June to December, 2014) that both variables were measured in Field survey 1. Bars not sharing the same letter are different (LS means tests, $p < 0.05$ ; [A] $n = 12$ for each combination of Depth x Month, except at the shallow station in September and November, and deep station in August, with $n = 10, 9,$ and $9,$ respectively; Tables B.1 and D1. [B] $n = 4$ for each combination of Depth x Month, except at the shallow station in June and the deep station in October, with $n = 2,$ and $3,$ respectively; Tables B.1 and D.2).	
<b>Figure 2.4</b>	37
Water flow speed at the shallow (12 m) sampling station from 28 July to 7 December, 2014. Water flow velocity was recorded with a Doppler current meter at 5 cm above the rhodolith bed at a rate of 64 readings $\text{min}^{-1}$ during the first 15	

min of every hour. Each data point is the average of the 960 readings in the in the  $x$ -,  $y$ -, and  $z$ -direction available for each hour (see section 2.2.2.1 for details about averaging of flow velocities into dimensionless flow speeds). Data gaps identified by arrows at the top are when the instrument was taken out for data readout and maintenance.

- Figure 2.5** Mean ( $\pm$ SE) density (A, B) or wet weight (C-I) of (A) large green sea urchins [*Strongylocentrotus droebachiensis*]; (B) large common sea stars [*Asterias rubens*]; (C, D) daisy brittle stars [*Ophiopholis aculeata*]; (E, F) mottled red chitons [*Tonicella marmorea*]; (G, H) small green sea urchins; and (I) small common sea stars on rhodoliths at the shallow (12 m) and deep (20 m) stations in the seven months (June to December, 2014) that rhodolith sediment load was measure in Field survey 1. Bars not sharing the same letter are different (LS means tests,  $p < 0.05$ ; see Appendix B for sample sizes across depths and months and Tables E.1 to E.6 for details of statistical analysis for each panel). Post-hoc comparisons (LS means tests) did not yield significant differences in pairwise comparisons among sampling months in (C) and (E) despite factor Month's significance in the corresponding ANOVAs (see section 2.2.5.3 for additional information about such infrequent outcomes). Letters above bars are therefore not presented in these two panels. 39
- Figure 2.6** Mean (+SE) movement of marked rhodoliths over five days (A) at the shallow [12 m], intermediate [16 m], and deep [20 m] sampling stations [data pooled across the three surveys]; and (B) in the three surveys; 1 = mid-November, 2 = late November, and 3 = early December [data pooled across the three sampling stations], in Field survey 2. Bars not sharing the same letter are different (LS means tests,  $p < 0.05$ ;  $n = 90$  for each bar in both panels; see Table 2.2 for justification of data breakdown). 45
- Figure 2.7** Water flow speed at the shallow (12 m) sampling station during the three late fall surveys in Field survey 2: (A) mid-November [13 to 18 November, 2014], (B) late November [27 November to 2 December], and (C) early December [3 to 7 December]. Water flow velocity was recorded with a Doppler current meter at 5 cm above the rhodolith bed at a rate of 64 readings  $\text{min}^{-1}$  47

during the first 15 min of every hour. Each data point is the average of the 960 readings in the in the  $x$ -,  $y$ -, and  $z$ -direction available for each hour (see section 2.2.2.1 for details about averaging of flow velocities into dimensionless flow speeds).

**Figure 2.8** Mean (+SE) movement of rhodoliths over 4 h in the presence or absence of green sea urchins (*Strongylocentrotus droebachiensis*) and common sea stars (*Asterias rubens*) in the mesocosm experiment (control = no urchins or sea stars). Bars not sharing the same letter among the first three treatments are different (LS means tests,  $p < 0.05$ ;  $n = 12$  for each bar). A one-tailed  $t$  test was used to compare rhodolith movement between the control treatment ( $n = 12$ ) and treatment with next higher average (presence of two sea stars; see section 2.2.5.3 for details of statistical analysis). 50

## LIST OF APPENDICES

	Page
<b>Appendix A</b> Comparison of water flow between shallow and deep stations	74
<b>Appendix B</b> Breakdown of number of observations used to model rhodolith sediment load	77
<b>Appendix C</b> Explanatory power of water flow and selection of best-fitting model	78
<b>Appendix D</b> Outcome of statistical analyses for Figure 2.3	83
<b>Appendix E</b> Outcome of statistical analyses for panels A to I in Figure 2.5	84

## **CO-AUTHORSHIP STATEMENT**

The work described in the present thesis was conducted by Kyle R. Millar with guidance from Patrick Gagnon, Dominique Robert, and Evan Edinger. Kyle R. Millar was responsible for field and laboratory data collection and analysis (with assistance by Patrick Gagnon) and contributed to modifications brought to the original design by Patrick Gagnon. All chapters were written by Kyle R. Millar with intellectual and editorial input by Patrick Gagnon. Any publication in the primary literature resulting from work in the present thesis and from complementary work not presented will be co-authored by Kyle R. Millar and Patrick Gagnon.

## **CHAPTER I**

### **GENERAL INTRODUCTION**

Hydrodynamic forces exert considerable influence on the structure and dynamics of shallow marine communities (Gaylord 1999, Kraufvelin et al. 2010, Blain & Gagnon 2013). The shallow subtidal zone is defined as the area below the lowest tide line that experiences disturbance due to wave action, and for many species waves and tidal currents delineate the boundaries they live within (Eckman et al. 2008). Some species are not capable of withstanding intense wave action, and can be dislodged or rendered incapable of foraging (Miller et al. 2007). Like in the intertidal zone, zonation in species assemblages exist in the subtidal driven by hydrodynamic forces as well as competition (Stotz et al. 2016). The shallow subtidal zone is exposed to oscillatory forces from wave action, in addition to uni- or bi-directional tidal forces and disturbance by storm events, and these forces are important drivers of species zonation and behaviour.

Rocky shores present particular challenges and opportunities for fauna and flora regarding wave action. Exposed bedrock is rarely homogeneous, and presents cracks, crevices, and roughened surfaces (Turra & Denadai 2006). Many macrophytes grip bedrock directly using holdfasts, and animals possess unique adaptations to avoid dislodgement (Xu et al. 2016). Similar to seaweeds, barnacles and bivalves attach directly to rocky surfaces and cluster with other individuals for strength (wa Kangeri et al. 2016). Other animals modify behaviour, such as marine snails seeking cracks for shelter in intense waves, or simply retreating to deeper waters to lessen the effect (Kemppainen et al. 2005). For other organisms, wave action can be beneficial, such as kelp species relying on dislodgement of herbivores by wave action (Lauzon-Guay & Scheibling 2007). As being dislodged can result in transport to unfavorable depths, being smashed against the shore or becoming

vulnerable to predation, all organisms of the shallow subtidal must cope with unfavorable hydrodynamic conditions.

Another challenge in the marine realm is falling sediments. Shorelines are the interface between marine and terrestrial ecosystems, and freshwater input is laden with organic and inorganic matter that is transported into the ocean and eventually settles on the seabed at various distances from points of disgorgement (Ryan et al. 2007). This matter is captured by filter feeders and detritivores and can form the basis of entire food webs (Drolet et al. 2004b, Tecchio et al. 2013). However, sediments can also cloud water, choke respiratory organs, and accumulate on exposed surfaces (Li et al. 2014). Sessile species are especially vulnerable to burial, as some lack the ability to relocate or remove sediment. Degree of wave exposure and tidal forces also drives sedimentation to a large degree as hydrodynamic forces re-suspend finer sediments, and can carry them to deeper waters (Julien 2010).

The size of sediment particles that can be re-suspended by hydrodynamic forces determines intertidal and subtidal substrate (Balsinha et al. 2009). In sheltered areas, mudflats can exist typically where nearby rivers discharge high volumes of fine particulate matter as these silts are easily washed away and collect near the mouth of the river (Dyer 2000). In semi-exposed areas where silts are typically washed away, sand sized grains can accumulate. In higher degrees of exposure, beaches are formed of larger and larger pebbles and eventually exposed bedrock dominates. On exposed rocky shores, there exist patterns of substrate that roughly correspond with these shore stages in the subtidal zone at deeper depths, with silts settling in deep waters and sand and pebbles below the exposed bedrock (Sibaja-Cordero et al. 2012). The type and degree of substrates present on a shore influence

species composition, as greater heterogeneity generally leads to greater species diversity (Ferrier & Carpenter 2009, Gingold et al. 2010).

A highly successful group in the shallow subtidal are coralline red algae. These algae have a thallus that is rigid due to deposits of calcium carbonate in cell walls, and are typically seen encrusting rocky surfaces (Sebens 1986, Dethier & Steneck 2001). They occur worldwide, with over 1600 species described, including a single freshwater occurrence (W. J. Woelkerling 1988, Žuljević et al. 2016). Coralline algae are divided in two groups: geniculate, which possess flexible joints between rigid calcareous sections, and non-geniculate, which lack flexible joints (Steneck 1986). Non-geniculate encrusting algae can produce entirely calcified branches that create highly heterogeneous surfaces on otherwise homogeneous surfaces.

Rhodoliths are free-living balls of calcareous algae, and are created either by sexual spores or asexual reproduction, generally through fragmentation (Freiwald 1995). Rhodoliths are long-lived and slow growing, with most growth estimates being less than  $2.7 \text{ mm year}^{-1}$  (Bohm et al. 1978, Bosence & Wilson 2003). Rhodoliths are tolerant to periods of covering by faster growing soft-tissued macrophytes as they possess starch reserves (Basso et al. 2009). They are tolerant to changes in temperature (Noisette et al. 2013), though differences in growth rates are observed between seasons in temperate waters (Steller et al. 2007). Even though they are relatively tolerant to salinity changes or heavy metals, fine or anoxic sediments are stressful and potentially lethal (Wilson et al. 2004). As rhodoliths are formed of high-magnesium calcium carbonate, they are vulnerable to ocean acidification (Nelson 2009). Rhodoliths are important as ecosystem engineers, as their complex tridimensional structure adds heterogeneity to an otherwise smooth sediment

bottom (Gurney & Lawton 1996). Teichert (2014) showed that rhodoliths, especially those with hollow centres, exhibit a greater diversity of taxa including algae, invertebrates, and fishes than comparable habitat lacking rhodoliths. Rhodoliths are themselves an alternate food source for certain species, including urchins (James 2000). Littler et al. (1995) described a mutualism between a species of crustose algae and a chiton, wherein the chiton cleaned away dead tissue and competing algae species. Due to high biodiversity in rhodolith beds, they have a vast potential for bioprospecting that remains largely uninvestigated (Amado-Filho & Pereira-Filho 2012). These factors all contribute to rhodoliths as a key habitat building species globally (Freiwald & Henrich 1994, Amado-Filho, Pereira-Filho, et al. 2012).

Rhodoliths typically form dense aggregations on sediment bottoms known as rhodolith beds (Freiwald & Henrich 1994). These beds exist worldwide and can cover large areas, with the biggest known bed spanning 20,900 km<sup>2</sup> along the coast of Brazil (Amado-Filho, Pereira-Filho, et al. 2012). Beds can be found in waters anywhere from a few meters deep (Basso et al. 2009) to over 150 m deep (Tsuji 1993a). Commercially and economically important species, such as the queen scallop, use rhodolith beds as a nursery habitat (Hall-Spencer et al. 2003), and rhodoliths themselves are harvested in France and Brazil as a soil additive (Grall & Hall-Spencer 2003, Amado-Filho & Pereira-Filho 2012). These beds play an important role in global calcium carbonate (CaCO<sub>3</sub>) budgets, as a square meter of bed can accumulate a kilogram of CaCO<sub>3</sub> in a year (Ryan et al. 2007, Amado-Filho, Moura, et al. 2012). When rhodoliths die, they crumble and create CaCO<sub>3</sub> sand that is available for use in the creation of new rhodoliths, or potentially buried as rhodoliths are well represented in the fossil record (Bosence 1983a, Riosmena-Rodríguez et al. 2012).

As rhodoliths are free-living and formed of relatively dense calcium carbonate, frequent rolling is likely needed for bed persistence. Rolling is thought to remove sediment on the rhodolith surface, reduce epiphytes, and facilitate maintenance of photosynthetic tissue on all surfaces (Foster 2001). The primary mechanisms for displacement are thought to be water motion, and the reworking of sediment particles by animals, a phenomenon known as bioturbation (Marrack 1999). The frequency of displacement is a delicate balance as too little displacement may lead to burial, overgrowth, and partial surface death, while too much could result in rhodoliths abrading against each other and the substrate, and fragmentation (Basso 1998, Basso et al. 2009). These processes may delineate the edges of a bed, with the upper boundary typically shaped by wave action, and the deeper boundary by the settling of fine silts (Steller & Foster 1995).

Factors and processes that regulate the structure, function, and stability of rhodolith beds are far less understood than those in long-studied coral reef, seagrass, and kelp bed (forest) systems (Foster 2001, Kaldy & Lee 2007, Montaggioni & Braithwaite 2009, Filbee-Dexter & Scheibling 2014). Experiments in rhodolith beds to date have largely been “snapshot”, examining singular portions of relatively isolated beds, with no or little replication over time (Riosmena-Rodriguez et al. 2017). Results are difficult to generalize among beds across spatial and temporal scales. Identifying factors that control the distributional limits (bathymetric and geographic) of rhodolith beds is difficult because of differences in hydrodynamics, animal populations, and their interrelationships. Longer-term studies across multiple spatial and temporal scales are needed to understand the dynamic processes that determine rhodolith bed boundaries.

Rhodolith beds in the northwest Atlantic have been known to exist since the 1960s, but the majority of studies to date have been descriptive in nature. Adey (1966) described several beds along the coast of Newfoundland and Labrador, and other investigated the primary species of coralline algae and their distribution (Adey & Adey 1973, Adey et al. 2005, Adey & Hayek 2011). Gagnon et al. (2012) carried out the first quantitative research about rhodolith bed structure and associated fauna. They compared rhodolith shape and dominant macro- and crypto-faunal species in two beds in Conception Bay, Newfoundland, and found that two species (the daisy brittle star *Ophiopholus aculeata* and the mottled red chiton *Tonicella marmorea*) represented over 82% of total invertebrates in both beds. Green sea urchins (*Strongylocentrotus droebachiensis*) and the common sea star (*Asterias rubens*) were commonly observed displacing at the surface of the rhodolith bed (Gagnon et al. 2012). Conception Bay experiences semi-diurnal tidal periods and is exposed to strong winter storms that frequently come from the north in the late Fall (Brodie et al. 1993). These factors, as well as sediment discharge from human activities and rivers, make this area interesting to investigate the factors leading to rhodolith bed persistence.

The respective role of wave action and bioturbation, as well as their interaction, on the reworking of rhodoliths is poorly understood. The goal of this research is to explore the relationship between rhodolith sediment loading and displacement by water motion and common macrofaunal species as it relates to the persistence of beds. Chapter II includes (1) a 7-month observational study of a rhodolith bed in eastern Newfoundland, relating sedimentation rate, water motion, and density and biomass of common cryptofauna and macrofauna to rhodolith sediment load; (2) a field survey measuring displacement of tracked rhodoliths at three depths within the bed and at three time periods; and (3) a

mesocosm experiment testing the rhodolith bioturbation potential of the green sea urchin (*Strongylocentrotus droebachiensis*) and the common sea star (*Asterias rubens*). Chapter III presents a summary of the main findings and their contribution to advancing knowledge about factors and processes that regulate the structure and function of rhodolith beds. It also discusses future research directions in this area.

## **CHAPTER II**

**INFLUENCE OF HYDRODYNAMIC ENVIRONMENT AND BIOTURBATION ON SEDIMENT**

**ACCUMULATION IN A NEWFOUNDLAND RHODOLITH BED**

## 2.1 INTRODUCTION

Sedimentation is the deposition on a physical barrier of suspended organic and inorganic particles (sediments) settling out of a water column (Wright et al. 2001, Julien 2010, Twichell et al. 2010). Marine sediments are an important food source for detritivores and filter feeders in benthic environments and their accumulation can create nutrient-rich depositional layers providing habitat and shelter (Dearborn et al. 1981, Hall 1994). However, sessile benthic organisms, in particular primary producers such as seagrasses and seaweeds, are vulnerable to excessive sedimentation occluding feeding and photosynthetic structures or interfering with recruitment, growth, and gaseous or nutrient exchange with the water column (Thomsen & McGlathery 2006, Cabaço & Santos 2007, Riul et al. 2008). Smothering or burial by sediments can be reduced or avoided when physical factors such as water flow or organisms remove or re-suspend sediments (Scheffer et al. 2003, Hinchey et al. 2006, Boer 2007). Bioturbation, broadly defined as transport processes carried out by animals that directly or indirectly affect sediment matrices, including both particle reworking and burrow ventilation is a widespread phenomenon that helps maintain biologically sustainable sedimentary balances in benthic systems (Dahlgren et al. 1999, Kristensen et al. 2012, Chen et al. 2016). Yet, increasing frequency and intensity of wind and wave storms, as well as accelerating coastal development, affect near-shore sediment regimes and increase the likelihood of destructive sedimentation, including the loss of primary producers (IPCC 2014).

Rhodoliths are red, benthic, non-geniculate coralline algae (Rhodophyta, Corallinaceae) that grow as free-living nodules (balls, branched twigs, or rosettes) from the low intertidal to depths >150 m in tropical to polar seas (see review by Foster 2001). They

are long-lived and slow-growing, with estimated longevity that can exceed 100 y and highest growth rates of only a few millimeters per year (Bohm et al. 1978, Bosence 1983b, Foster 2001). Rhodoliths can form extensive CaCO<sub>3</sub> bio-factories, known as rhodolith beds (aggregations), with the largest bed, ~20 900 km<sup>2</sup>, along the coast of Brazil (Foster 2001, Amado-Filho, Moura, et al. 2012). In part because of their high structural complexity, rhodolith beds typically contain highly diverse assemblages of ecologically and economically important invertebrate and fish species (e.g. Kamenos 2004, Kamenos et al. 2004, Gagnon et al. 2012). Most studies of rhodolith beds to date have focused on quantifying their distribution and biodiversity, with only a few studies of the factors and processes that regulate their structure, function, and stability (Kamenos et al. 2004, Riosmena-Rodríguez et al. 2012, Riosmena-Rodríguez et al. 2017).

According to Foster (2001), rhodolith beds typically develop in environments where light is high enough for rhodolith growth, and water motion is strong enough to prevent burial by sediment but not so high or directional as to cause destruction or transport out of favorable growth conditions. Although theoretically sound, this paradigm has remained largely untested since its inception over 15 years ago. Movement of rhodoliths within a bed, which can help discharge some of the settling sediments, can be attributed to two main factors: hydrodynamic forces and bioturbation (Riosmena-Rodríguez et al. 2017). Hydrodynamic forces include tidal currents, oscillatory waves, and disturbance by extreme wave storms, which are all presumably affecting mainly the upper limit of rhodolith distribution (Tsuji 1993b, Marrack 1999, Basso et al. 2009). Bioturbation in rhodolith beds is generally attributed to activities of a variety of echinoderms and benthic fishes (Prager & Ginsburg 1989, James 2000). The importance of bioturbation in preventing rhodolith

burial, and how it may differ spatially within a bed, is relatively unknown and difficult to quantify (Prager & Ginsburg 1989, Piller & Rasser 1996, Marrack 1999). Moreover, the relative importance of the hydrodynamic environment and bioturbation on rhodolith movement is poorly understood and likely differs spatially, temporally, and geographically.

The first published account of occurrence of rhodolith beds in the northwestern Atlantic dates back the mid-1960s (Adey 1966), followed by only a handful of studies describing the main coralline species that form rhodoliths and coarse geographical distribution of the beds across this vast region (Adey & Adey 1973, Bosence 1983b, Adey et al. 2005, Adey & Hayek 2011). The study by Gagnon et al. (2012) focusing on two subtidal rhodolith (*Lithotamnion glaciale*) beds off the coasts of Holyrood and St. Philip's in southeastern Newfoundland, is the first quantitative analysis of rhodolith morphology, associated cryptofaunal and macrofaunal abundance and diversity, and organization as beds in the subarctic, northwestern Atlantic. Because the bed in St. Philip's is relatively large (~0.25 km<sup>2</sup>), extends across a depth range of ~10 to 25 m, and is located at ~300 m from the mouth of a river, it may be under the influence of a broad range of water flows and sedimentological processes (Gagnon et al. 2012). The daisy brittle star, *Ophiopholis aculeata*, and mottled red chiton, *Tonicella marmorea*, are the two dominant rhodolith cryptofauna, accounting for ~82% of total numbers of invertebrates in the bed (Gagnon et al. 2012). The former is a suspension feeder, whereas the latter is a grazer, and hence together these organisms can filter sediments falling out of the water column and scrape the surface of rhodoliths. Dominant macroinvertebrates present on the surface of the bed include the common sea star, *Asterias rubens*, and green sea urchin, *Strongylocentrotus droebachiensis* (Gagnon et al. 2012). By moving on the beds, both species may alter the

positions of rhodoliths and their sediment load, therefore possibly acting as bioturbators. Given these characteristics, the rhodolith bed in St. Philip's represents an excellent system to study sedimentological aspects and gain a better understanding of the factors and processes that affect rhodolith bed distribution and stability in general.

In the present study, two surveys in the rhodolith bed in St. Philip's, as well as one laboratory mesocosm experiment with two dominant mobile invertebrates from this bed, were used to characterize, parse, and model spatial and temporal variation in rhodolith sediment load and movement among presumably important abiotic and biotic factors. Specifically, one survey tracked and modeled changes in rhodolith sediment load over seven months as a function of water flow, sedimentation, and the abundance of dominant rhodolith cryptofauna and macrofauna near the upper and lower margins of the bed. The other survey examined movement of rhodoliths and water flow over three weeks near the centre and upper and lower margins of the bed. The mesocosm experiment tested the ability of common sea star and green sea urchin in displacing rhodoliths. Collectively, these surveys and experiment were designed to test the hypotheses that: (1) water flow and the abundance of at least a few dominant rhodolith cryptofauna and macrofauna influence the amount of sediment on rhodoliths; (2) rhodolith movement within a bed is inversely related to depth; and (3) sea urchins cause greater rhodolith movement than sea stars.

## **2.2 MATERIALS AND METHODS**

### **2.2.1 Study site**

The present study was carried out from June to December 2014 in a rhodolith (*Lithothamnion glaciale*) bed spanning ~0.25 km<sup>2</sup> across depths of 10 to 25 m off the coast of St. Philip's on the south shore of Conception Bay, Newfoundland, Canada (47°35' 30.9" N, 52°53' 35.2" W; Figure 2.1a,b). Rhodoliths in this bed are relatively small (length of longest axis on average ~6 cm) and predominantly spheroidal (Gagnon et al. 2012) (Figure 2.1c,d). Their corrugated surface holds high densities (up to ~2000 individuals m<sup>-2</sup> of bed) of the daisy brittle star, *Ophiopholis aculeata*, and mottled red chiton, *Tonicella marmorea* (Gagnon et al. 2012). Dominant macroinvertebrates moving on the surface of the bed include the green sea urchin, *Strongylocentrotus droebachiensis*, and common sea star, *Asterias rubens* (Gagnon et al. 2012).

### **2.2.2 Rhodolith sediment load (Field survey 1)**

The amount of sediment covering the surface of rhodoliths, hereafter termed “sediment load”, and its relationship with environmental variability was assessed by tracking changes over seven months in the (1) quantity of sediment falling out of the water column; (2) density of dominant, mobile invertebrate macrofauna on rhodoliths; and (3) biomass of dominant rhodolith cryptofauna, at depths of 12 and 20 m in the bed. These depths were chosen because they correspond roughly to the respective upper and

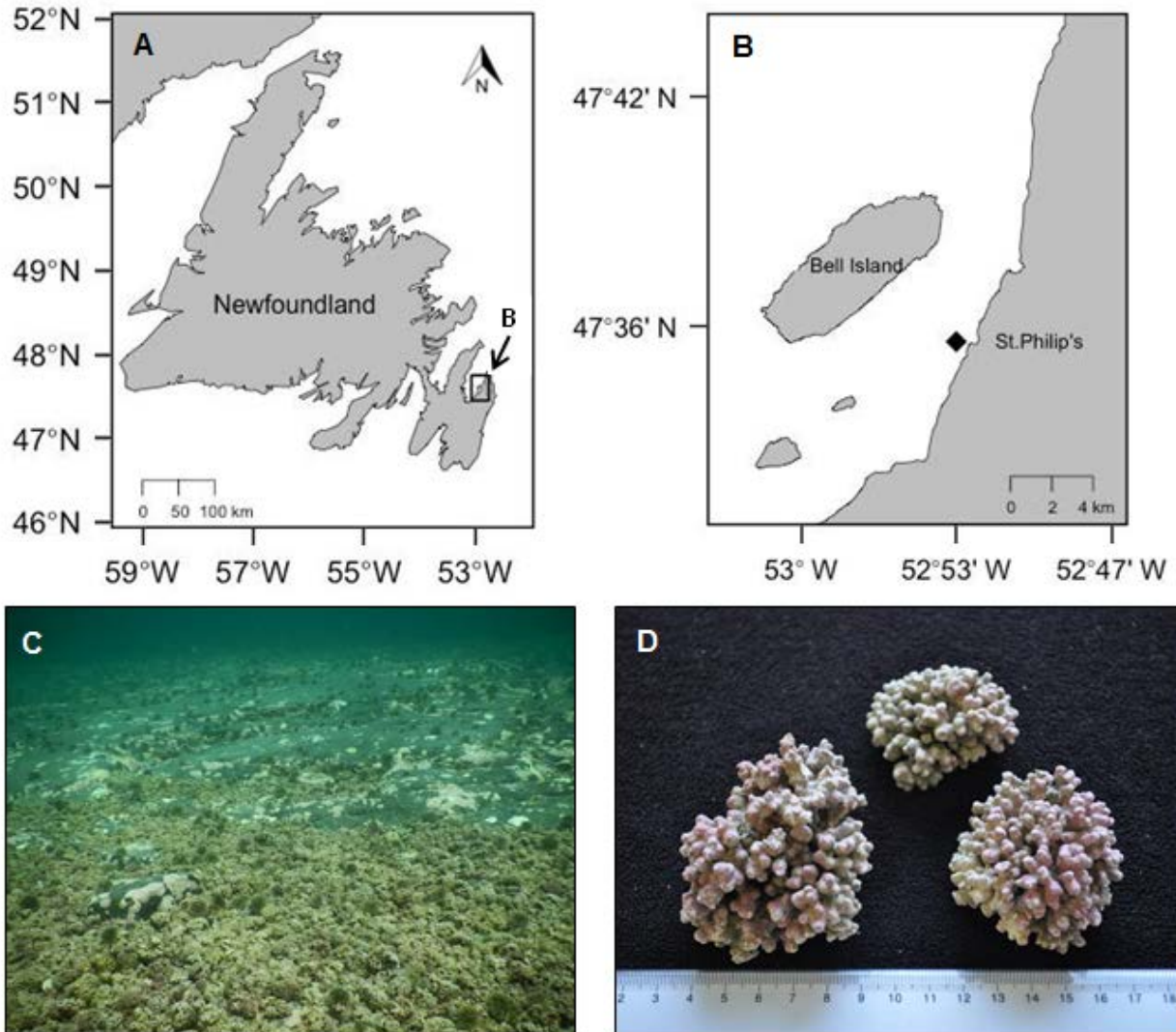


**Figure 2.1.** Maps of (A) Newfoundland [eastern Canada] and (B) eastern Conception Bay showing the location of the studied rhodolith bed [diamond] off St. Philip's. (C) Transition [5 m across] between urchin [*Strongylocentrotus droebachiensis*] barrens [upper half] and rhodolith [*Lithothamnion glaciale*] bed [lower half] at a depth of ~10 m [Photo: David Bélanger]. (D) Size [centimeter scale] and shape [primarily spheroidal] of representative rhodoliths from the bed [Photo: Patrick Gagnon].

lower margins of the bed, with presumed differences in water flow (higher at 12 than 20 m) and sediment load (lower at 12 than 20 m). For simplicity and accuracy, the concept of rhodolith sediment load in the present study refers strictly to the amount of sediment on the surface of rhodoliths at a given point in time. The concept therefore differs from that of “load” in the geological literature used to describe sediment particles in a flowing fluid either transported along the physical confine of the fluid flow (bed load), or suspended within a given volume of fluid (suspended and wash loads; Julien 2010).

Sediment load was measured once every 21-40 days (seven times in total) from 11 June to 9 December, 2014. On each sampling event, 120 rhodoliths of comparable size were haphazardly hand collected by divers within a large (~50 x 50 m) georeferenced area of the bed at each depth. The present study was primarily concerned with sediment settling out of the water column. Only rhodoliths whose underside was not wedged in sediments and did not release a plume of sediments upon removal from the bed were retained to reduce the likelihood of sampling both benthic and deposited waterborne sediment. Rhodoliths were carefully removed to not alter sediment load and transported to the surface in large (3.78 L), sealed plastic bags (10 rhodoliths per bag for a total of 12 bags). Bags of rhodoliths with their water content were transported in large containers filled with seawater to the Ocean Sciences Centre (OSC) of Memorial University of Newfoundland. Upon arrival at the OSC (<5 hours after collection), bags were transferred to 330-L holding tanks supplied with ambient flow-through seawater pumped in from a depth of ~5 m in the adjacent embayment of Logy Bay.

The content of each bag was processed using the following procedure. Each rhodolith was vigorously shaken for 30 seconds within the bag to release sediment in the water. Water and total sediment load from the 10 rhodoliths was then filtered with a vacuum pump (model 0211-V45F-G8CX; Gast) through a 25- $\mu\text{m}$  filter paper (Grade 114 Wet-Strengthened Qualitative Filter Paper; Whatman). Sediment retained was air dried for 24 hours at 60°C in a drying oven (model GO1390A-1; Thermo Scientific). Sediment dry weight was then determined by subtracting the original dry weight of the filter paper from the dry weight of the filter paper and its sediment load as measured using a scale with a precision of  $\pm 0.001$  g (PB503-S/FACT; Mettler Toledo).

Rhodoliths sampled inevitably differed in shape, size, and orientation on the seabed despite efforts to minimize such variation during collection. As a result, a part of the variation in rhodolith sediment load among the 12 groups of 10 rhodoliths was likely caused by differences in the total amount of rhodolith surface on which sediment settled, with larger rhodoliths likely trapping more sediment than smaller ones. To account for this potential bias and standardize sediment loads, total sediment weight for each group of 10 rhodoliths was divided by the sum of all surface areas of those same 10 rhodoliths. The total surface area of each rhodolith was estimated by relating the length of the longest, intermediate, and shortest axes, measured with a caliper with a precision of  $\pm 0.1$  cm, with the Knud Thomsen approximation for a general ellipsoid with least relative error (at most 1.061%):

$$S \approx 4\pi \left( \frac{(ab)^p + (ac)^p + (bc)^p}{3} \right)^{1/p}$$

where  $S$  is the surface area,  $p = 1.6075$ , and  $a$ ,  $b$ , and  $c$  are half the lengths of the longest, intermediate, and shortest axes, respectively (Klamkin 1971). Gagnon et al. (2012) used the lengths of the longest, intermediate, and shortest axes and simple mathematical relationships described by Graham & Midgley (2000) to approximate rhodolith shape in the same bed examined in the present study, and concluded that rhodoliths were predominantly spheroidal. Because calculation of rhodolith surface areas in the present study required greater accuracy, and none of the rhodoliths collected were true spheres, the Knud Thomsen approximation for a general ellipsoid was deemed superior to any other methods of approximation.

#### **2.2.2.1 Water flow**

Water flow velocity,  $u$ ,  $v$ , and  $w$  (in the  $x$ -,  $y$ -, and  $z$ -direction, respectively) at the shallow (12 m) station, was measured from 28 July to 7 December, 2014 with a Doppler current meter (Vector Current Meter; Nortek). The instrument was attached vertically to a frame anchored to the seabed. Velocity at 5 cm above the rhodolith bed was recorded at a rate of 64 readings  $\text{min}^{-1}$  during the first 15 min of every hour (for a total of 960 readings  $\text{hr}^{-1}$ ). This sampling regime, termed “burst sampling”, is commonly used in oceanographic studies to estimate hydrodynamic conditions over long time scales (Lowe et al. 2005, Thomson & Emery 2014). Velocity in each direction was averaged across each block of 15 min. The resulting three mean velocities for each time block were then averaged into a single, overall, directionless flow speed (Smith 1994).

Only one Doppler current meter was available, precluding continuous measurement of flow simultaneously at the deep (20 m) station. To determine whether flow velocity differed between both stations, the instrument was temporarily moved once every two or three weeks (depending on availability) to the deep station. It was left there for ~1.5 h to ensure flow velocity was recorded uninterruptedly over 15 min, and relocated to the shallow station for further recording. The instrument was brought to the OSC once a month for precautionary data readout and maintenance, and redeployed at the shallow station generally within the following two or three days, resulting in a few data gaps throughout the survey. Water flow at both stations was deemed similar (Appendix A). Accordingly, preliminary investigation of the relationship between water flow and rhodolith sediment load was restricted to the shallow station because of the finer temporal resolution in flow regime available for this station (see Statistical Analysis).

#### **2.2.2.2 Waterborne sediments**

Sediments falling through the water column were collected from 2 May to 7 December, 2014, with sediment traps at both stations. Each trap consisted of a 30-cm long PVC pipe with an internal diameter of 5.08 cm and a plastic cap tightly affixed to one end. Accordingly, length was approximately six times greater than diameter, which is above the minimum 5:1 ratio needed to prevent re-suspension of trapped sediments in high-energy wave and current environments (White 1990, Storlazzi et al. 2011). The traps were fastened, open end facing upwards at a height of 1 m above the bed, to a thin (1.9 cm in diameter) metal rod secured to a 15-kg cinder block placed horizontally on the bed. Four

traps located 1 to 4 m from one another were used simultaneously at each station. Every 23 to 40 days, divers tightly capped the open end of all traps and swapped them for empty ones. Traps with sediments were then brought to the laboratory to determine the amount of sediments. The sediment content of each trap was filtered and dried with the same methodology used for determining rhodolith sediment load (see section 2.2.2). Sedimentation rate for each trap was calculated by dividing sediment dry weight by the surface area of the trap aperture (20.3 cm<sup>2</sup>) and number of days the trap was at the station (Storlazzi et al. 2011).

### **2.2.2.3 Mobile invertebrate macrofauna**

A preliminary survey of the rhodolith bed at both stations indicated that the green sea urchin, *Srongylocentrotus droebachiensis*, and common sea star, *Asterias rubens*, were by far the dominant invertebrate macrofauna displacing on the bed. Green sea urchins can move rhodoliths (James 2000), whereas several species of sea stars, including *A. rubens*, are effective bioturbators on soft-sediment bottoms (Gaymer et al. 2004, Scheibling & Metaxas 2008). Accordingly, both species were chosen to examine the influence of mobile invertebrate macrofauna on rhodolith sediment load. The density of urchins and sea stars at both stations was measured every 19 to 38 days from June 11 to December 7, 2014, with the following procedure. On each sampling day at each station, divers swam with a quadrat (30 x 30 cm) and a digital camera (PowerShot D30, Canon) above the bed over a straight distance of ~75 m. Every 2 or 3 m, the diver holding the quadrat closed their eyes (to avoid bias) and deposited the quadrat on the bed. The quadrat was then photographed. Twenty

(20) to 30 photo quadrats were acquired at each station. The mean density of each species on each sampling day for each station was determined from visual counts in the 20 to 30 photo quadrats of urchins and sea stars with a test diameter >2 cm and body diameter (length of the longest axis between two opposing arm tips) >5 cm (minimum detectable sizes on the imagery), respectively.

#### **2.2.2.4 Rhodolith cryptofauna**

A complementary study of the same rhodolith bed showed the dominant rhodolith cryptofauna are the daisy brittle star, *Ophiopholis aculeata*, and mottled red chiton, *Tonicella marmorea*, together representing respectively 82% and 78% of the total number and biomass of invertebrates (Gagnon et al. 2012). Juvenile *S. droebachiensis* and *A. rubens* were the next two most abundant (density and biomass) cryptofaunal species (Gagnon et al. 2012), which is consistent with preliminary observations in the present study. Accordingly, these four species were chosen to examine the influence of rhodolith cryptofauna on rhodolith sediment load. All *O. aculeata*, *T. marmorea*, *S. droebachiensis*, and *A. rubens* were extracted with probes and forceps from the same rhodoliths sampled for sediment load (see section 2.2.2).

Most brittle stars were firmly attached to rhodoliths with the bulk of their body deeply recessed within rhodolith surface cavities, making it virtually impossible to extract individuals without tearing body parts. Accordingly, biomass of each of the four species was quantified because it was deemed a more accurate estimator of their potential influence on sediment load than density. Rhodoliths were fractured into pieces as required to ensure complete extraction of biomass. Total wet weight per species of all individuals (whole and

fragments) from each of the twelve groups of 10 rhodoliths collected at each station on each sampling event was determined with a scale (same as in section 2.2.2) with a precision of 0.001 g, and averaged for each group of rhodoliths.

### **2.2.3 Rhodolith movement in the field (Field survey 2)**

To verify the assumption that rhodolith movement occurs in natural habitats, while testing the hypothesis that movement is inversely related to depth, a 3-week survey of changes in the location of marked rhodoliths across an 8-m depth gradient was carried out at the study site, at ~150 m from both stations in Field survey 1. The survey was partitioned in three runs of 5 days each in late fall 2014, when wave action in southeastern Newfoundland typically picks up (Brodie et al. 1993, present study) and is more likely to affect the distribution of unattached benthos like rhodoliths: (1) 13 to 18 November [hereafter termed “mid-November”]; (2) 27 November to 2 December [late November]; and (3) 2 to 7 December [early December].

On 23 October, 2014, divers hand collected ~250 non-nucleated, average-sized rhodoliths at depths of 14 to 18 m. Rhodoliths were transported to the OSC where they were individually weighted, and the length of their longest, intermediate, and shortest axes was measured as detailed above (see section 2.2.2). Dimensions from each rhodolith were then aggregated using the spreadsheet TRIPLOT (<http://www.lboro.ac.uk/microsites/research/phys-geog/tri-plot/>) developed by Graham & Midgley (2000) from the pioneering work by Sneed & Folk (1958) to assign each rhodolith to one of three major shapes (spheroidal, discoidal, or ellipsoidal). Spheroidal rhodoliths

weighing between 15 and 35 g and with longest axis between 3 and 6 cm were dried for 36 hours at 60°C in a drying oven (GO1390A-1; Thermo Scientific). They were subsequently marked (spray painted bright orange) to facilitate relocation underwater.

Marked rhodoliths were transported back to the study site on 13 November, 2014, and deployed at depths of 12 (shallow), 16 (intermediate), and 20 (deep) m according to the following procedure. At each depth, divers created two rows of five groups of four rhodoliths, for a total 20 rhodoliths per row and 40 rhodoliths per depth. The four rhodoliths in each group were deposited on top of the rhodolith bed, in a 20 x 20-cm square (with one rhodolith per corner) centred in a 50 x 50-cm reference frame to standardize distances among marked rhodoliths. Thin metal rods marked with small pieces of bright colored flagging tape were driven into the sediments underlying the bed, at two opposing corners of the frame to permanently mark its location and orientation. The frame was moved along the row and deposited every 1 m to lay out the remaining four groups of marked rhodoliths and permanently mark each new frame location and orientation with additional metal rods. The second row of rhodoliths was created in the same way and paralleled the other row at a distance of ~2 m.

Each frame and associated rhodoliths was photographed from above with a digital camera (PowerShot D30; Canon) at the beginning and end of each run. The two images of a same frame were superimposed and cropped as needed to correct for differences in camera angle with Image J (Schneider et al. 2012). Pieces of bright tape affixed to the sides of the frame at known distances from the corners were used to calibrate and standardize distances within and between superimposed images. The net distance between each marked

rhodolith's initial and final positions in the imagery was averaged for each group of four rhodoliths belonging to a same frame, yielding 40 estimates of rhodolith movement per depth per run, for a total of 360 estimates throughout the survey. The same marked rhodoliths and frame locations and orientations were used at all three depths in the three runs.

A preliminary experiment was conducted to determine whether the paint used to mark the rhodoliths influenced the frequency at which the two predominant macrofaunal species in the rhodolith bed, the green sea urchin, *Strongylocentrotus droebachiensis*, and common sea star, *Asterias rubens*, contacted rhodoliths. Trials were conducted at the OSC in a shallow (43 cm deep), 31 x 31-cm glass tank filled with seawater. Sixteen (16) rhodoliths were disposed in a circle (28 cm in diameter) on the bottom of the container. One contiguous half of the circle was composed of dried, unpainted rhodoliths, and the other contiguous half of rhodoliths dried and painted as explained above. Each trial began with the placement of one urchin (4-5 cm in t.d.) or one sea star (10-15 cm in b.d.) in the centre of the circle of rhodoliths, and ended when the urchin or sea star had contacted one of the rhodoliths, whose identity (painted or not) was then noted. Twenty (20) trials were run for each species, each with new seawater and a new urchin or sea star. The position of unpainted and painted rhodoliths within each contiguous half of the circle, as well as the placement of each half within the circle (e.g. top versus bottom or left versus right portions of the circle), were systematically alternated from one trial to the next. There was no difference between the proportion of urchins that contacted unpainted (55%) and painted (45%) rhodoliths ( $\chi^2=0.2$ ,  $p=0.65$ ). There was also no difference between the proportion of sea stars that contacted unpainted (50%) and painted (50%) rhodoliths ( $\chi^2=0$ ,  $p=1$ ).

Rhodolith painting was therefore deemed to have no influence on the frequency of contacts by dominant macrofauna in the bed, and hence unlikely to bias rhodolith movement in the field as measured with the approach described above.

#### **2.2.4 Rhodolith movement by dominant macrofauna (Mesocosm experiment)**

Casual, qualitative observations of dominant macrofauna in the rhodolith bed at St. Philip's (and other beds in Newfoundland) suggested that green sea urchins, and to a lesser extent common sea stars, moved a few rhodoliths over various distances while displacing. To quantitatively demonstrate this phenomenon, while testing the hypothesis that urchins cause greater rhodolith movement than sea stars, a laboratory mesocosm experiment was carried out in which changes in the location of rhodoliths in the presence or absence of urchins and sea stars were tracked. The four treatments tested were: (1) presence of one urchin and one sea star; (2) presence of two urchins; (3) presence of two sea stars; and (4) no urchins and no sea stars. The first three treatments were designed to isolate and compare any differential effects of sea stars and urchins, whereas the last treatment was used as a control for sea star and urchin effects.

The experiment was carried out with spheroidal rhodoliths (3-6 cm in length, longest axis), urchins (4-5 cm in t.d.), and sea stars (10-15 cm in b.d.) hand collected by divers at depths of 10 to 15 m from the bed in St. Philip's on 18 and 27 November, 2014. Organisms were transported to the OSC in large containers filled with seawater and transferred upon arrival (<4 h after collection) to 330-L holding tanks supplied with flow-through sea water pumped in from a depth of ~5 m in the adjacent embayment, Logy Bay. These urchin and sea star size classes were chosen to ensure all individuals were sexually

mature (Nichols & Barker 1984, Himmelman & Dutil 1991, Munk 1992), therefore eliminating potential behavioral differences between mature and non-mature individuals; and because they were the most readily available in the bed at the time of collection. All urchins and sea stars were starved for one week prior to experimentation to standardize hunger and activity levels (Scheibling & Hatcher 2007, St-Pierre & Gagnon 2015). Only urchins and sea stars that clung or displaced readily in the tanks, indicating normal activity of the podia, were used.

Trials were carried out in plastic trays (35 x 30 x 12 cm [L, W, H]) submerged right below the water surface in 75-L glass tanks (62 x 31 x 43 cm [L, W, H]) supplied with  $\sim 1 \text{ L min}^{-1}$  of flow-through seawater (one basket per tank; Fig. 2.2). Perforations (1 cm in diameter) every 1.5 cm along the sides of the trays enabled continuous water exchange between the tray and tank. The bottom of each tray was covered with a 1-cm-thick layer of sediment collected near the upper margin of the rhodolith bed in St. Philip's, on top of which nine rhodoliths were deposited in a 3 x 3 grid arrangement, with a distance of  $\sim 2.5$  cm between adjacent rhodoliths. Each trial lasted 4 h and began with the addition (or not) of urchins and sea stars to each tray. Urchins and sea stars were gently deposited between the first and second, and second and third rhodoliths that formed the middle row of three rhodoliths in each grid (Figure 2.2). Each basket was photographed from above with a digital camera (PowerShot D30; Canon) at the onset of trials, and every 30 min thereafter until the end. Images were analyzed with Image J v1.48 (Schneider et al. 2012) to determine each rhodolith's total movement, defined as the sum of the linear distances

moved from one image to the next. Total movement was averaged across the nine rhodoliths of a same tray.

Trials were conducted in 24 tanks spatially blocked in six groups of four tanks each. Each tank in each block was randomly assigned one of the four experimental treatments, enabling six independent replicates of each treatment simultaneously. The experiment was repeated two times, with a first run on 25 November and a second run on 4 December, yielding 12 replicates per treatment (n=48). Water temperature in the tanks was recorded every 15 min with a temperature logger (HOBO Pendant; Onset Computer Corporation). Mean temperature during trials in the first and second runs was respectively  $5.17 \pm 0.01$  and  $3.47 \pm 0.02$  °C. All urchins and sea stars were used only once.

## **2.2.5 Statistical analysis**

### **2.2.5.1 Field survey 1**

A two-way ANOVA with the fixed factors Depth (shallow [12 m] and deep [20 m] stations) and Month (the seven months in which rhodolith sediment load was measured; June to December) was used to test for differences in rhodolith sediment load (RSL) between shallow and deep rhodoliths over time (n=168). The analysis was applied to the raw data. Six (6) two-way ANOVAs with the fixed factors Depth (shallow and deep stations) and Month (seven months; June to December, 2014) were used to test for differences in density or biomass of dominant rhodolith macrofauna (two species) and cryptofauna (four species) between shallow and deep rhodoliths over time (n=332 or

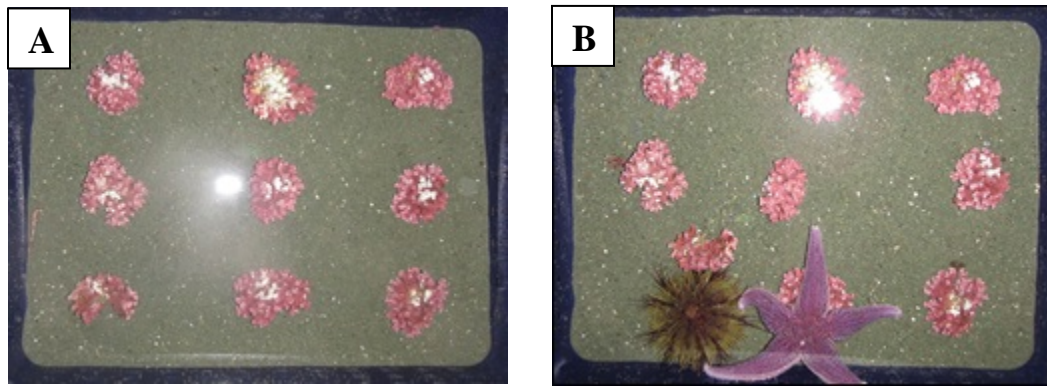


**Figure 2.2.** Experimental set-up used to quantify rhodolith movement by green sea urchins (*Strongylocentrotus droebachiensis*) and common sea stars (*Asterias rubens*) (Mesocosm experiment). (A) Location of the nine rhodoliths on the sediment layer covering the experimental area [35 x 30 cm] prior to adding one urchin and one sea star in a trial with both organisms. (B) Location of the rhodoliths, urchin, and sea star at the end [t=4 h] of the same trial. Rhodoliths were marked at the top (white speckles) to facilitate tracking. The white spots in respectively the middle and top of panels A and B are glare from the camera flash used to photograph the experimental area.

158 depending on species). These analyses were also applied to the raw data.

Multiple linear regression analysis (Eberly 2007) was used to examine the relationship between RSL and environmental variability. Several stepwise regression models were required to identify the best model fit, as judged by comparing variation ( $\Delta$ ) in the Akaike Information Criterion (AIC) from one model to the next: the larger the  $\Delta$ AIC between two models, the more dissimilar these models with the best model assigned the lowest AIC (Burnham & Anderson 2004). The AIC was preferred over the Bayesian Information Criterion (BIC) because the former introduces a smaller penalty term for the number of model parameters, therefore reducing the likelihood of overfitting models. AIC was also deemed more adequate than the corrected Akaike Information Criterion (AIC<sub>c</sub>) in accommodating the relatively large sample sizes in the models examined (n=43 to 1445), as recommended by Burnham & Anderson (2004). As per Singer & Willett (2003), a  $\Delta$ AIC of 4 or more between two models was considered a large enough difference to declare both models different in their respective explanatory powers.

Explanatory variables included (or not) in the various models were: (1) significant flow speed [SFS]; (2) sedimentation rate [SR]; (3) density of adult sea urchins on rhodoliths [DSU]; (4) density of adult sea stars on rhodoliths [DSS]; (5) biomass of cryptic brittle stars [BBS]; (6) biomass of cryptic mottled red chitons [BRC]; (7) biomass of cryptic sea urchins [BSU]; (8) biomass of cryptic sea stars [BSS]; (9) sampling station [S]; and (10) sampling month [M]. All variables were treated as random, with the exception of S, M, and their interaction, which were treated as fixed. The average of the highest one-third (1/3) of the mean hourly flow speed values recorded over set periods of time, hereafter

termed significant flow speed (SFS) per analogy to significant wave height (SWH) used broadly in oceanographic studies (Pinet 2000), was used in all models that incorporated water flow as an explanatory variable. Accordingly, SFS in the present study is an approximately monthly time-integrated proxy of flow conditions likely to induce the largest variation in rhodolith sediment load.

Because of logistical considerations limiting data collection, the number of observations, and hence sample sizes, varied slightly among sampling stations and months. Two sediment traps were lost at the shallow station in June and data from one sediment trap at the deep station in October was omitted because of a likely obstruction to sediment catchment by a dead urchin found in the trap. In most months, DSU and DSS could not be determined from a few low-quality photo quadrats. A few bags of rhodoliths were also lost, precluding measurement of RSL, BBS, BRC, BSU, and BSS (See sample sizes details in Appendix B). RSL values in the various models were tested against DSU, DSS, BBS, BRC, BSU, and BSS values, which were all measured on the same day as RSL, approximately monthly during seven months. RSL values were also simultaneously tested against SFS and SR values indicative of water flow and sedimentation in the month or so leading to RSL measurement. For example, shallow RSL values on 3 September, 2014 were tested against the average of the highest 1/3 of mean hourly flow speed values (292 values), and average of SR values (four values), acquired since the previous measurement of RSL on 28 July, 2014 (Table B.1). Because replication among factors was uneven (an unbalanced design as per Quinn & Keough [2002]), variance among model terms was inevitably heterogeneous. Accordingly, an extension of Welch's test included in the R package Companion to Applied

Regression ('car') (Fox & Weisberg 2011) was used to adjust degrees of freedom and protect against increased Type I error (Wilcox 2011).

The explanatory power of SFS on rhodolith sediment load, limited to the shallow station and for the period during which SFS data was available (see section 2.2.2.1 and Appendix A for explanation), was investigated with stepwise regression analysis as a first step to determining the best model fit. SFS was deemed unimportant to rhodolith sediment load, and hence was excluded from further analyses of data from both sites throughout the entire survey (Appendix C). Stepwise regression analysis with data from both sites throughout the entire survey indicated the best-fitting model to rhodolith sediment load included all candidate variables, except SR (Appendix C). This model ( $RSL = DSU + DSS + BBS + BRC + BSU + BSS + S + M + S * M$ ) is scrutinized in the results section.

#### **2.2.5.2 Field survey 2**

A nested ANOVA (Quinn & Keough 2002) with the fixed factor Depth (the three depths at which rhodolith movement was quantified: 12, 16, and 20 m), random factor Frame (the 10 frames sampled at each depth) nested within Depth, and fixed factor Run (the three 5-day runs over which rhodolith movement was quantified: mid-November, late November, and early December) was used as a first step to test for differences in rhodolith movement among frames (n=90). There was no significant effect of the factor Frame nested within Depth ( $F_{27,54}=1.296$ ,  $p=0.206$ ). A two-way ANOVA with the fixed factors Depth (12, 16, and 20 m) and Run (the three 5-day runs) with data pooled across frames was therefore used to test the effects of depth and sampling period on rhodolith movement

(n=90). Both analyses were treated as particular cases of the generalized linear model (negative binomial) to correct for heteroscedasticity and deviation of residuals from normality detected in the first place with a classical linear model (Venables & Ripley 2002).

### **2.2.5.3 Mesocosm experiment**

A two-way ANOVA with the fixed factors Block (the six blocks of four tanks assigned one of the four experimental treatments), and Run (the two experimental runs with six blocks of tanks each) was used as a first step to test for differences in rhodolith movement among experimental blocks and runs (n=36). There was no significant effect of the factor Block ( $F_{5,24}=0.287$ ,  $p=0.916$ ) and Run ( $F_{1,24}=2.934$ ,  $p=0.099$ ). A one-way ANOVA with the fixed factor Macrofauna (three out of the four combinations of presence and absence of sea stars and urchins) with data pooled across Block and Run was therefore used to test for differences in rhodolith movement by urchins and sea stars (n=36). Unlike the three other treatments, rhodolith movement in the control treatment (no sea stars and no urchins) was null (see Results), potentially artificially influencing the outcome of both analyses. Data from the control treatment were excluded in both analyses to avoid such a bias. These data were instead compared to those from the treatment with the next higher average (presence of two sea stars) with a one-tailed  $t$  test (two-sample assuming unequal variances). Both ANOVAs were applied to the raw data.

In all regressions and ANOVAs, homogeneity of the variance and normality of the residuals were respectively verified by examining the distribution of the residuals and the normal probability plot of the residuals (Snedecor & Cochran 1994). In ANOVAs, Tukey HSD multiple comparison tests (comparisons based on least-square means; Sokal & Rohlf

2012) were used to detect differences among levels within a factor. In the analysis of rhodolith macrofauna and cryptofauna, these comparisons tests did not detect significant differences in the biomass of daisy brittle stars and mottled red chitons among sampling months identified as significant in the associated ANOVAs (Figure 2.5 C and E and corresponding Tables E.3 and E.4). This outcome is infrequent, yet possible given that post-hoc analyses examine pairwise comparisons while ANOVAs examine the difference between all treatment levels. A significance level of 0.05 was used in all analyses. All the analyses were carried out in R 3.0.2 (R Core Team 2014). All means are presented with standard errors (mean  $\pm$  SE) unless stated otherwise.

## **2.3 RESULTS**

### **2.3.1 Field survey 1**

Rhodolith sediment load (RSL) varied with depth among months (a significant interaction between the factors Depth and Month, Table D.1), ranging from  $1.2 \pm 0.1$  mg sediment  $\text{cm}^{-2}$  rhodolith in December in deep (20 m) rhodoliths to  $5.3 \pm 0.6$  mg sediment  $\text{cm}^{-2}$  rhodolith in September in shallow (12 m) rhodoliths. It was twice higher (a significant difference) in shallow than deep rhodoliths at the onset of the survey in June, but otherwise similar at both depths in any given month until the end in December (Figure 2.3). There was a similar seasonal trend in RSL at both depths, with a gradual increase from July to September (shallow) or June to August (deep), followed by a steeper decrease until the end (Figure 2.3). Peak RSL in September at 12 m and in

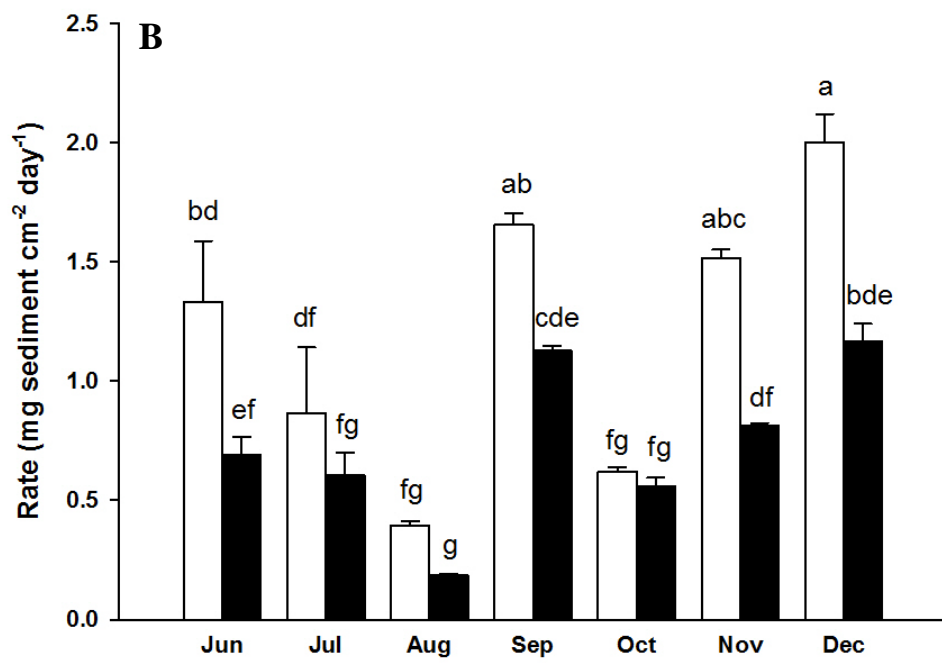
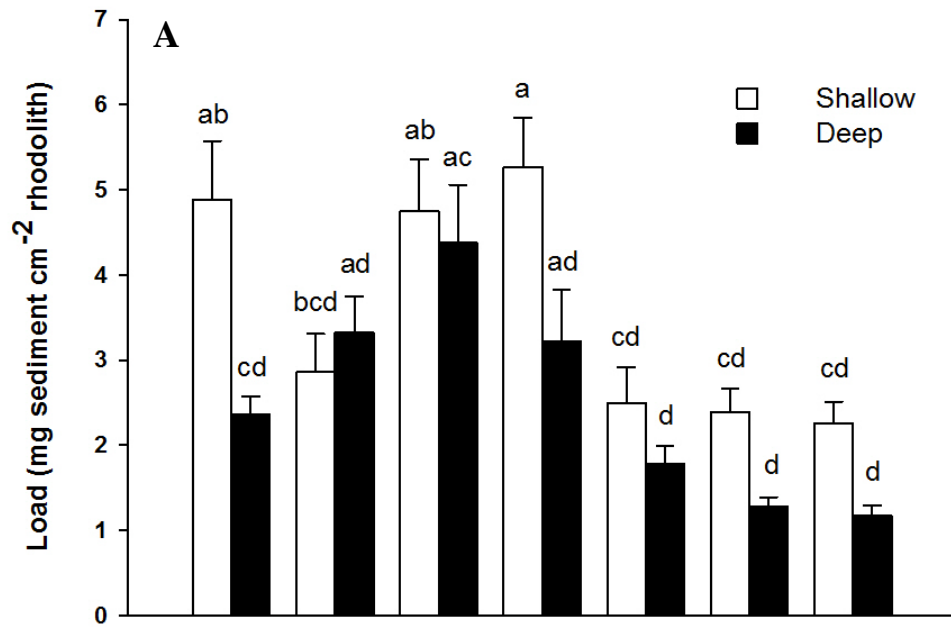


**Figure 2.3.** Mean (+SE) (A) rhodolith sediment load (dry weight) and (B) sedimentation rate (dry weight) at the shallow (12 m) and deep (20 m) stations in the seven months (June to December, 2014) that both variables were measured in Field survey 1. Bars not sharing the same letter are different (LS means tests,  $p < 0.05$ ; [A]  $n = 12$  for each combination of Depth x Month, except at the shallow station in September and November, and deep station in August, with  $n = 10, 9,$  and  $9,$  respectively; Tables B.1 and D.1. [B]  $n = 4$  for each combination of Depth x Month, except at the shallow station in June and the deep station in October, with  $n = 2$  and  $3,$  respectively; Tables B.1 and D.2).

August at 20 m was at least twice higher than the lowest RSL values at both depths in December (both differences significant, Figure 2.3). Sedimentation rate (SR) also varied with depth among months (a significant interaction between the factors Depth and Month Table D.2), ranging from  $0.19 \pm 0.00$  mg sediment  $\text{cm}^{-2} \text{day}^{-1}$  in August in deep rhodoliths to  $2.00 \pm 0.12$  mg sediment  $\text{cm}^{-2} \text{day}^{-1}$  in December in shallow rhodoliths (Figure 2.3). Yet, preliminary simple linear regression analysis showed there was no relationship between RSL and SR in both shallow ( $R^2 = -0.182$ ,  $p = 0.794$ ) and deep ( $R^2 = 0.189$ ,  $p = 0.182$ ) rhodoliths.

Water flow speed in the shallow portion of the bed was generally low throughout the survey, ranging from  $0.001 \text{ m s}^{-1}$  on 18 October, to  $0.301 \text{ m s}^{-1}$  on 8 November (Figure 2.4). Except for the first part of October when there was a lull, water flow speed was generally lowest and least variable until the third week of August, not exceeding  $0.155 \text{ m s}^{-1}$ , and gradually increased while becoming more variable until the end of the survey, with at least six episodes of a few hours with speeds  $>0.2 \text{ m s}^{-1}$  in November (Figure 2.4). Water flow speed in the deep and shallow portions of the bed was similar (Appendix A).

Analysis of rhodolith macrofauna and cryptofauna showed that the density of large green sea urchins and common sea stars moving on the surface of the rhodolith bed did not vary appreciably throughout the 7-month survey, though was respectively 37% and 36% higher in the shallow than deep portions of the bed (Figure 2.5, Tables E.1 and

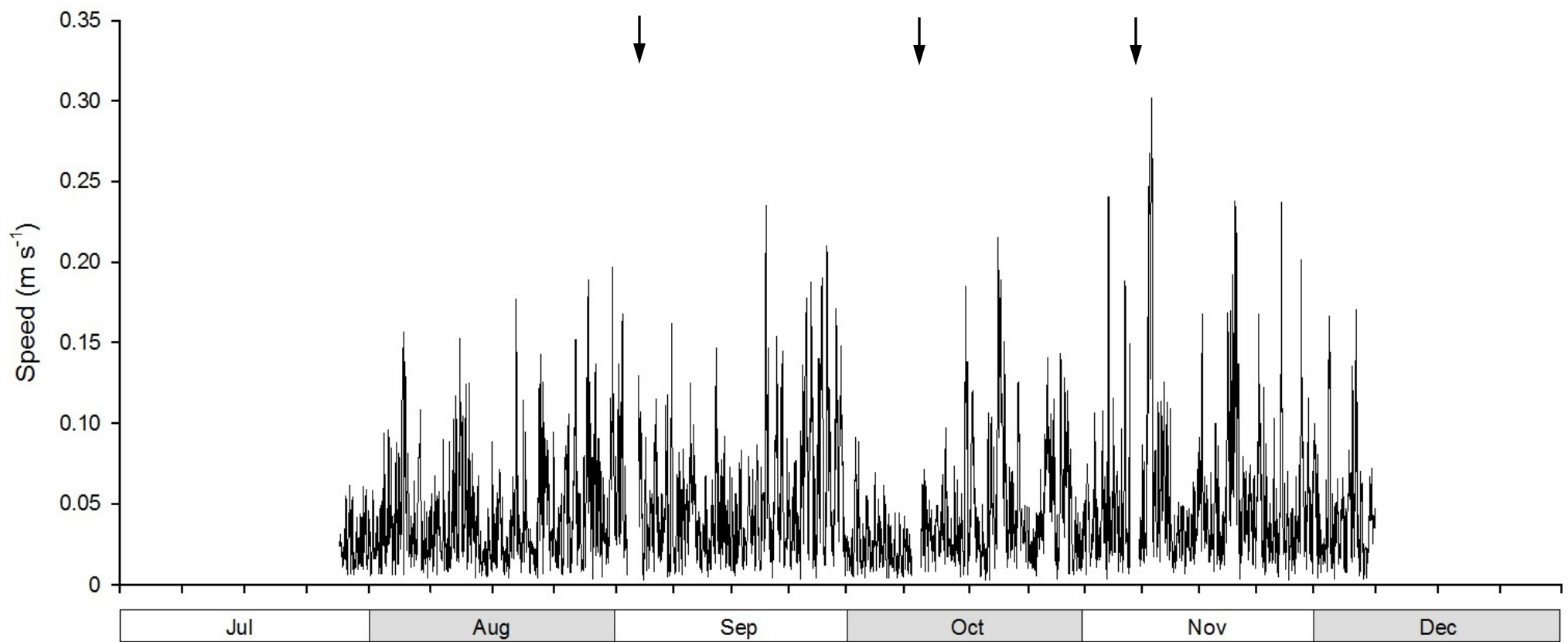


**Figure 2.4.** Water flow speed at the shallow (12 m) sampling station from 28 July to 7 December, 2014. Water flow velocity was recorded with a Doppler current meter at 5 cm above the rhodolith bed at a rate of 64 readings  $\text{min}^{-1}$  during the first 15 min of every hour. Each data point is the average of the 960 readings in the in the  $x$ -,  $y$ -, and  $z$ -direction available for each hour (see section 2.2.2.1 for details about averaging of flow velocities into dimensionless flow speeds). Data gaps identified by arrows at the top are when the instrument was taken out for data readout and maintenance.

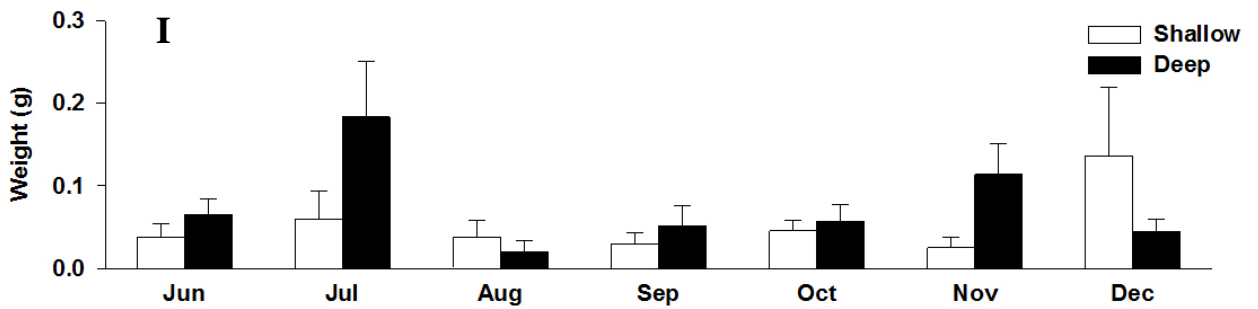
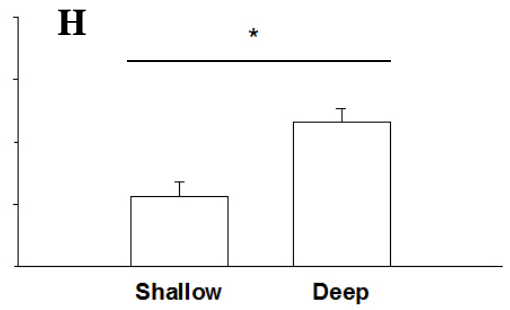
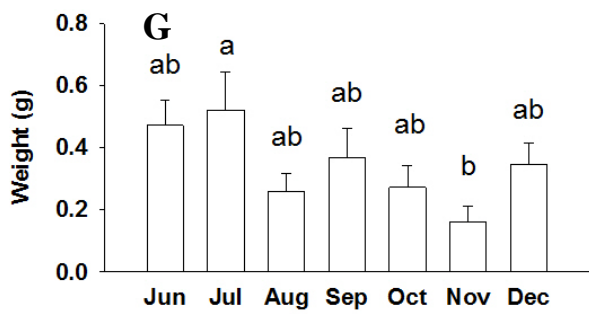
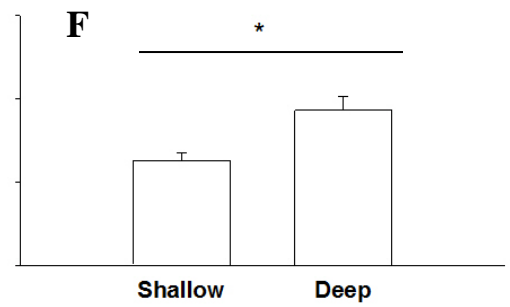
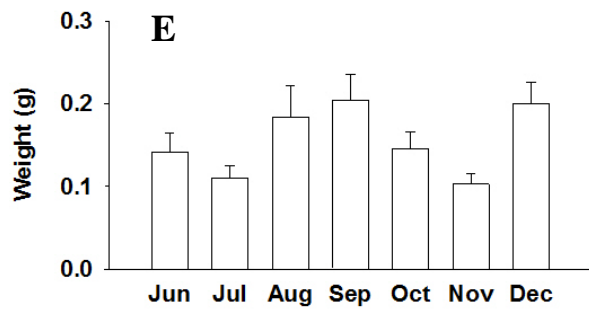
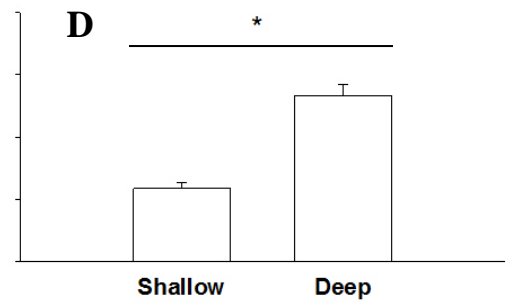
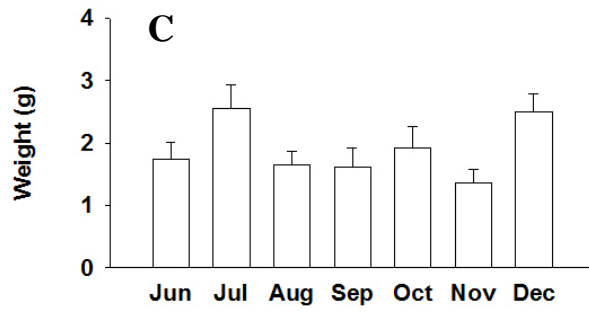
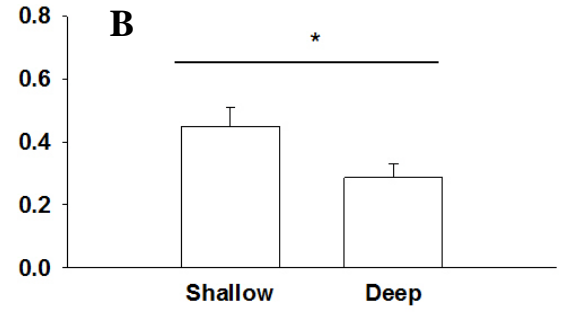
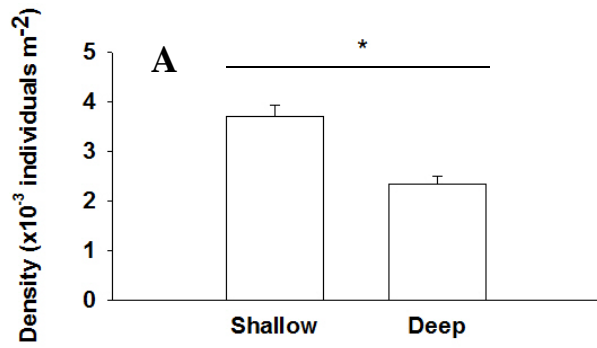


**Figure 2.5.** Mean ( $\pm$ SE) density (A, B) or wet weight (C-I) of (A) large green sea urchins [*Strongylocentrotus droebachiensis*]; (B) large common sea stars [*Asterias rubens*]; (C, D) daisy brittle stars [*Ophiopholis aculeata*]; (E, F) mottled red chitons [*Tonicella marmorea*]; (G, H) small green sea urchins; and (I) small common sea stars on rhodoliths at the shallow (12 m) and deep (20 m) stations in the seven months (June to December, 2014) that rhodolith sediment load was measure in Field survey 1. Bars not sharing the same letter are different (LS means tests,  $p < 0.05$ ; see Appendix B for sample sizes across depths and months and Tables E.1 to E.6 for details of statistical analysis for each panel). Post-hoc comparisons (LS means tests) did not yield significant differences in pairwise comparisons among sampling months in (C) and (E) despite factor Month's significance in the corresponding ANOVAs (see section 2.2.5.3 for additional information about such infrequent outcomes). Letters above bars are therefore not presented in these two panels.

E.2). In contrast, biomass of daisy brittle stars, mottled red chitons, and small green sea urchins within rhodoliths cavities varied significantly with time and depth independently (Tables E.3 to E.5). Brittle star biomass peaked in July and December and was at least 23% lower in the other months. It was also twice as high in deep than shallow rhodoliths (Figure 2.5). Chiton biomass was highest in August, September, and December, and 37% higher in deep than in shallow rhodoliths (Figure 2.5). Urchin biomass peaked in June and July, and was twice as high in deep than shallow rhodoliths (Figure 2.5). Biomass of small sea stars within rhodoliths cavities did not vary with time or depth (Table E.6), being generally low throughout the survey (Figure 2.5).

Stepwise regression analyses examining changes in Akaike Information Criterion (AIC) from one model to the next eliminated significant flow speed (SFS) and sedimentation rate (SR) as explanatory variables of RSL (Appendix C). The best-fitting model to data from both stations throughout the entire survey was:

$$\text{RSL} = \text{DSU} + \text{DSS} + \text{BBS} + \text{BRC} + \text{BSU} + \text{BSS} + \text{S} + \text{M} + \text{S} * \text{M}$$

where DSU and DSS are the density of large green sea urchins and common sea stars moving on rhodoliths, respectively; BBS, BRC, BSU, and BSS are the biomass (wet weight) of daisy brittle stars, mottled red chitons, small green sea urchins, and small common sea stars within rhodoliths cavities, respectively; S is the sampling station (deep or shallow), and M is the sampling month (June to December) (Appendix C). This model explained 38% of the variation in RSL ( $R^2=0.381$ ,  $p<0.001$ ). RSL was inversely related to biomass of cryptic brittle stars and small sea stars, yet both factors explained only a small proportion (<3%) of the variation in RSL (Table 2.1). RSL varied significantly between shallow and deep rhodoliths and over time both in the analysis of trends in RSL as

**Table 2.1.** Summary of multiple linear regression analysis (applied to raw data) examining the effect of the eight variables included in the best fitting-model of rhodolith sediment load in Field survey 1. DSU = density of large green sea urchins on rhodoliths; DSS = density of large common sea stars on rhodoliths; BBS = biomass (wet weight) of daisy brittle stars within rhodoliths interstices; BRC = biomass of mottled red chitons within rhodoliths interstices; BSU = biomass of small green sea urchins within rhodoliths interstices; BSS = biomass of small common sea stars within rhodoliths interstices; S = sampling station (shallow [12 m] or deep [20 m]); M = sampling month (June to December, 2014) (n=1461).

Source of variation	<i>Df</i>	MS	F-value	<i>p</i>	<i>R</i> <sup>2</sup>
DSU	1	9.154	3.78	0.054	0.006
DSS	1	0.041	0.02	0.896	-0.006
BBS	1	0.196	0.08	0.002	0.027
BRC	1	0.397	0.16	0.776	-0.006
BSU	1	24.763	10.24	0.686	-0.004
BSS	1	9.881	4.08	0.045	0.012
S	1	33.526	13.86	<0.001	0.066
M	6	27.987	11.57	<0.001	0.273
S*M	6	5.860	2.42	0.029	0.379
Error	139	2.419			
Corrected total	158				

mentioned above (Table D.1, Figure 2.3) and in the model relating RSL to environmental variables (Table 2.1).

### **2.3.2 Field survey 2**

Analysis of data from Field survey 2 showed that movement of marked rhodoliths varied among sampling depths and surveys independently (Table 2.2). Movement was at least 2.5 times higher in shallow (12 m deep) rhodoliths than in intermediate (16 m) or deep (20 m) rhodoliths (Figure 2.6). It was also at least 3.5 times higher in mid-November than in late November and early December (Figure 2.6). Instantaneous water flow speed (WFS) at 12 m was relatively low, not exceeding  $0.2 \text{ m s}^{-1}$  across the three surveys, and appeared generally more variable in late November (Table 2.3, Figure 2.7). Mean water flow speed was similar among the three surveys, ranging from  $0.039 \text{ m s}^{-1}$  in mid-November to  $0.044 \text{ m s}^{-1}$  in late November (Table 2.3). However, significant flow speed (SFS) in late November ( $0.087 \text{ m s}^{-1}$ ) was significantly higher than in mid-November, which in turn was similar to SFS in early December (Table 2.3).

### **2.3.3 Mesocosm experiment**

Rhodolith movement in the mesocosm experiment varied markedly among the various combinations of presence and absence of common sea stars and green sea urchins (one-way ANOVA:  $F_{2,33}=13.046$ ,  $p<0.001$ ). Movement was 46% higher in the presence of two urchins than in the presence of one urchin and one sea star, which in turn was two

**Table 2.2.** Summary of two-way ANOVA (generalized linear model with negative binomial distribution) examining the effect of Depth (12, 16, and 20 m) and Run (three surveys: 1 = mid-November, 2 = late November, and 3 = early December) on movement of marked rhodoliths in Field survey 2 (see section 2.2.3 for a description of the survey).

Source of variation	<i>df</i>	$\chi^2$	<i>p</i>
Depth	2	71.453	<0.001
Run	2	118.420	<0.001
Depth x Run	4	3.563	0.468

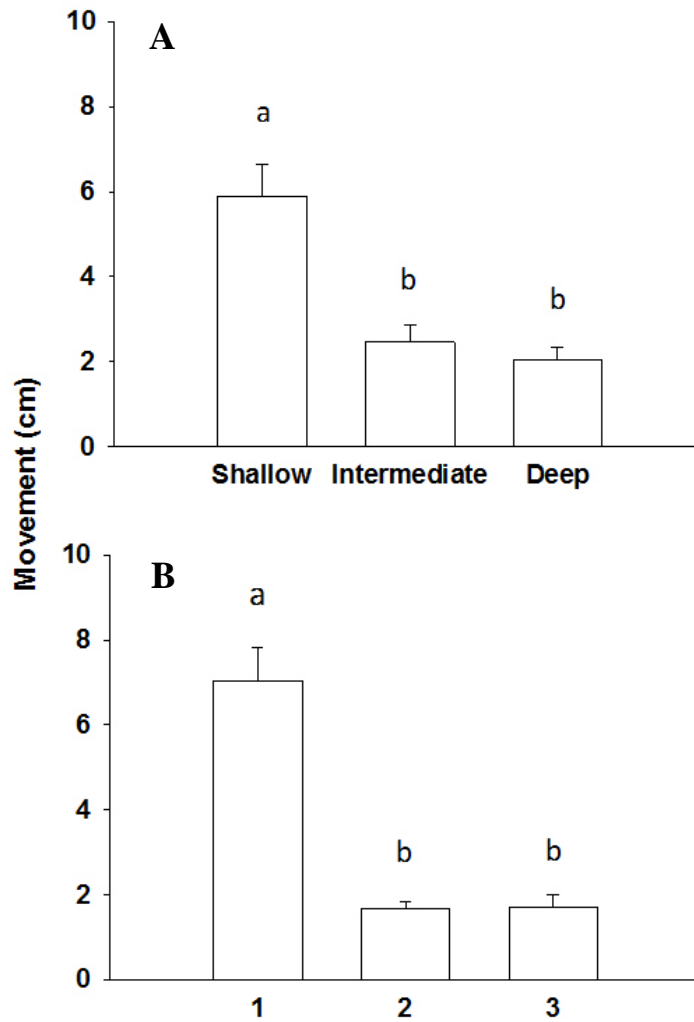


**Figure 2.6.** Mean (+SE) movement of marked rhodoliths over five days (A) at the shallow [12 m], intermediate [16 m], and deep [20 m] sampling stations [data pooled across the three surveys]; and (B) in the three surveys; 1 = mid-November, 2 = late November, and 3 = early December [data pooled across the three sampling stations], in Field survey 2. Bars not sharing the same letter are different (LS means tests,  $p < 0.05$ ;  $n = 90$  for each bar in both panels; see Table 2.2 for justification of data breakdown).

**Table 2.3.** Mean water flow speed (WFS), peak WFS, and significant flow speed (SFS) at the shallow (12 m) sampling station during the three late fall surveys in Field survey 2. Water flow velocity was recorded with a Doppler current meter at 5 cm above the rhodolith bed at a rate of 64 readings min<sup>-1</sup> during the first 15 min of every hour. Each data point is the average of the 960 readings in the in the *x*-, *y*-, and *z*-direction available for each hour (see section 2.2.2.1 for details about averaging of flow velocities into dimensionless flow speeds). Mean WFS is the average of all the hourly speed values, whereas SFS is the average of the highest 1/3 of the speed values.

Survey	Mean WFS ± Standard deviation (m s <sup>-1</sup> )	Peak WFS (m s <sup>-1</sup> )	SFS ±Standard deviation (m s <sup>-1</sup> )
Mid-November	0.039 ± 0.025	0.167	0.066 ± 0.023 <sup>b</sup>
Late November	0.044 ± 0.039	0.200	0.087 ± 0.040 <sup>a</sup>
Early December	0.041 ± 0.028	0.169	0.071 ± 0.027 <sup>ab</sup>
One-way ANOVA <sup>1</sup>	F <sub>2,348</sub> =0.944, p=0.390	-----	F <sub>2,114</sub> =4.884, p=0.009

<sup>1</sup>Both ANOVAs applied to raw data.

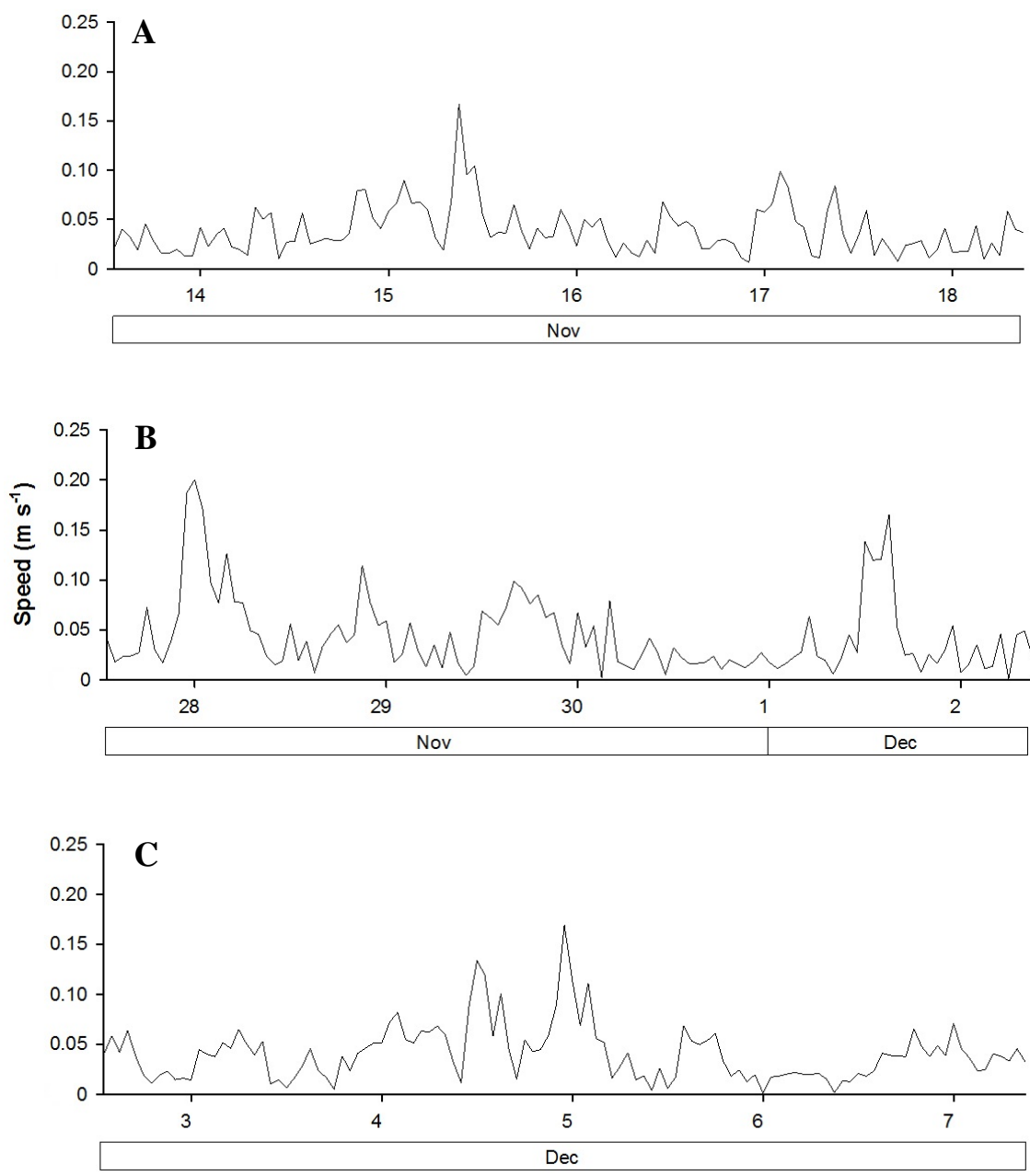


**Figure 2.7.** Water flow speed at the shallow (12 m) sampling station during the three late fall surveys in Field survey 2: (A) mid-November [13 to 18 November, 2014], (B) late November [27 November to 2 December], and (C) early December [3 to 7 December]. Water flow velocity was recorded with a Doppler current meter at 5 cm above the rhodolith bed at a rate of 64 readings  $\text{min}^{-1}$  during the first 15 min of every hour. Each data point is the average of the 960 readings in the in the  $x$ -,  $y$ -, and  $z$ -direction available for each hour (see section 2.2.2.1 for details about averaging of flow velocities into dimensionless flow speeds).

orders of magnitude higher than in the presence of two sea stars (Figure 2.8). As expected, movement in the absence of sea stars and urchins (control treatment) was null, yet was also virtually identical to that in the presence of two sea stars (Figure 2.8), indicating that the ability of sea stars to move rhodoliths was much lower than that of urchins.

## **2.4 DISCUSSION**

The two field surveys and laboratory mesocosm experiment provide strong evidence that rhodolith sediment load in the Newfoundland rhodolith bed studied was largely mediated by activities of a few numerically dominant benthic invertebrates. Rhodoliths were distributed across a depth range within which water flow did not vary appreciably and was likely too weak to induce rhodolith movement that could help remove sediments falling through the water column. Sedimentation appeared too low to bury rhodoliths or to overcome the anti-burial effect of rhodolith movement and surface cleaning by invertebrates. In a seminal review of knowledge about rhodolith biology and ecology, Foster (2001) proposed that control of rhodolith bed distribution lie along a continuum ranging from physical processes such as hydrodynamic forces and sedimentation, to biological processes such as bioturbation. Findings in the present study downplay the importance of hydrodynamic forcing as a mechanism regulating rhodolith sediment load, while elevating that of bioturbation.

### **Hydrodynamic environment**

Rhodoliths in the 7-month survey (Field survey 1) were sampled at the upper (12 m depth) and lower (20 m) margins of the rhodolith bed because of presumed

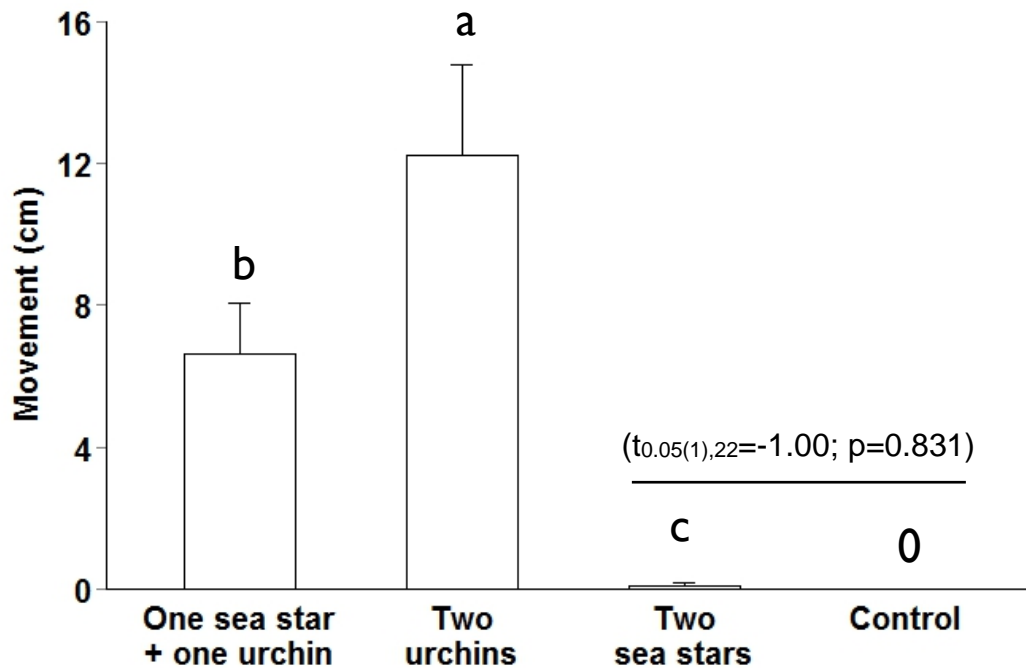


**Figure 2.8.** Mean (+SE) movement of rhodoliths over 4 h in the presence or absence of green sea urchins (*Strongylocentrotus droebachiensis*) and common sea stars (*Asterias rubens*) in the mesocosm experiment (control = no urchins or sea stars). Bars not sharing the same letter among the first three treatments are different (LS means tests,  $p < 0.05$ ;  $n = 12$  for each bar). A one-tailed  $t$  test was used to compare rhodolith movement between the control treatment ( $n = 12$ ) and treatment with next higher average (presence of two sea stars; see section 2.2.5.3 for details of statistical analysis).

depth-related differences in water flow regimes potentially affecting rhodolith sediment load (RSL). Interestingly, water flow regimes, even during that time of year (September to December) when wave energy typically increases in southeastern Newfoundland (Brodie et al. 1993, Blain & Gagnon 2013, Frey & Gagnon 2016), did not differ between depths. In fact, water flow was generally low throughout the survey, with a few peaks between 0.2 and 0.3 m s<sup>-1</sup> at 12 m that lasted only a few hours in November. In a study of the relationship between water motion and rhodolith displacement in the Gulf of California, Marrack (1999) showed that oscillatory water flow of at least 0.25 to 0.30 m s<sup>-1</sup> was required to induce rhodolith movement along the shallow (4.5 m) margin of a rhodolith bed. Rhodoliths in the latter study were about half the size of those in the present study, while being more spherical (Marrack 1999). It is therefore unlikely that the predominantly low water flows in the present study caused slight movement, <6 cm in five days, of heavier and flatter rhodoliths at 12, 16, and 20 m depths (Field survey 2).

Several findings support the notion that factors other than water flow mediated rhodolith sediment load (RSL) and movement. First, AIC model selection eliminated significant flow speed and sedimentation rate as explanatory variables of variation in RSL, retaining only factors containing information about spatial and temporal variation in the abundance of dominant rhodolith cryptofauna and macrofauna (see below). Second, movement of rhodoliths was thrice higher in mid- than late November, yet SFS was significantly higher in late than mid-November. Like water flow, sedimentation rate was relatively low, <2.3 mg cm<sup>-2</sup> day<sup>-1</sup>, throughout the survey at both depths sampled. Regression analysis also showed sedimentation rate and rhodolith sediment load were unrelated. These results strongly suggest that the bed extends naturally across a depth range

where hydrodynamic forces and the amount of sediments falling through the water column do not exceed levels that could alter the physiognomy of the bed via rhodolith fragmentation or burial, and basically switch the system from being biologically to physically driven. In other words, the bed appears to be located in an area where physical forcing was, at least during the 7 months (June to December) that the survey lasted, a much weaker determinant of rhodolith bed structure and stability than the animals inhabiting the bed.

Steller et al. (2009) report rapid burial and death of rhodoliths experimentally moved from within to below the lower margin of a bed in the Gulf of California. This finding is consistent with frequently invoked, but largely untested assumption that rhodolith beds typically develop in environments where water motion or bioturbation are strong enough to move rhodoliths within beds, preventing burial by sediments or biofouling, but not so high as to cause destruction (Steller & Foster 1995, Marrack 1999, Ballantine et al. 2000, Ryan et al. 2007). The present study provides the first quantitative demonstration that beds need not be exposed to threshold hydrodynamic conditions to avoid burial. It shows that beds can simply occur in areas where burial is unlikely to occur because of low sedimentation rates, in which case select resident bioturbators appear to suffice to maintain RSL below quantities that could alter rhodolith growth and survival (Wilson et al. 2004, Hall-Spencer et al. 2006, Riul et al. 2008).

### **Bioturbation**

Bioturbation (*sensu* Kristensen et al. 2012) is frequently proposed as a key process generating rhodolith movement in rhodolith beds (Foster 2001). However, since Marrack's

pioneering demonstration of bioturbation in a Californian rhodolith bed (Marrack 1999), only a handful of studies have quantitatively authenticated this phenomenon. For example, James (2000) studied diet, movement, and covering behaviour in the sea urchin *Toxopneustes roseus* in Californian rhodolith beds. He noted that urchins were often carrying live and dead pieces of rhodoliths on their aboral surface when displacing on the bed, or digging themselves into the bed creating pits up to 10 cm deep (James 2000). A similar phenomenon was casually observed at the upper and lower margins of the bed in the present study, with adult-sized (>2 cm in test diameter) green sea urchins, *Strongylocentrotus droebachiensis*, slowly plowing rhodoliths while displacing on the surface of the bed. The laboratory mesocosm experiment demonstrated the considerable ability of adult-sized green sea urchins in moving rhodoliths on a layer of sediments, while showing the near-complete inability of the next most abundant mobile macroinvertebrate in Newfoundland rhodolith beds, the common sea star, *Asterias rubens*. Both species use tens of podia to displace, but unlike the common sea star, the green sea urchin also moves large numbers of spines as it displaces, often bracing them into cracks and crevices to gain purchase (Frey & Gagnon 2016). Moreover, adult-sized common sea stars like those in the present study are considerably larger than rhodoliths and their five arms largely conform to the shape of objects on which they displace. Consequently, displacement of the latter is on top of multiple rhodoliths simultaneously, which largely prevents rhodolith movement, instead of in between rhodoliths like green sea urchins, which are as large or smaller than rhodoliths and can easily relocate them.

The present study also provides the first quantitative demonstration of differences in the ability of presumed bioturbators to move rhodoliths, while exploring quantitative

relationships between RSL and the abundance of bioturbators in rhodolith bed systems. Modeling showed that RSL was inversely related to biomass of cryptic daisy brittle stars (*Ophiopholis aculeata*) and small common sea stars populating rhodolith interstices. However, there was no clear relationship between RSL and biomass of adult-sized common sea stars and green sea urchins. These findings, together with those outlined above, have several important implications. First, bioturbation in rhodolith beds operates at several scales, with cryptofaunal species sometimes playing a greater role than macrofaunal species in modulating RSL. As explained, the best-fitting model to data from both depths sampled excluded water flow speed and sedimentation rate as explanatory variables of RSL. In the bed studied, activities of small brittle stars and sea stars appeared sufficient to maintain RSL under good control. Gagnon et al. (2012) quantified the abundance of daisy brittle stars within rhodoliths in the bed studied:  $\sim 900$  individuals  $m^{-2}$ . Red mottled chiton (*Tonicella marmorea*) was the next most abundant rhodolith cryptofauna with  $\sim 750$  individuals  $m^{-2}$  (Gagnon et al. 2012), yet there was no clear relationship between RSL and chiton biomass in the present study. One cryptofaunal species (brittle star) therefore appeared to play a dominant role in regulating RSL, whereas another co-occurring species (chiton) did not despite being nearly equally abundant. Drolet et al. (2004b) showed that daisy brittle stars often relocate on a daily cycle. Presumably, such frequent displacements, together with consumption of mainly waterborne organic sediments trapped with highly motile arms (Drolet et al. 2004a), were enough to swipe uncaught sediments off the surface or rhodoliths.

Second, species can be effective rhodolith bioturbators during certain portions of their life cycle or below threshold rhodolith densities. The microcosm experiment showed

that adult-sized common sea stars did not move rhodoliths while displacing, yet small, cryptic individuals significantly altered RSL in the bed. The experiment also showed that green sea urchins easily moved a few rhodoliths spaced out on a layer of sediment, yet did not affect RSL in the bed. With  $\sim 860$  rhodoliths  $m^{-2}$  (Gagnon et al. 2012), the bed contained a much higher density than in the experiment. Rhodoliths in the bed often formed tight patches of interlocked individuals, and hence movement of rhodoliths by urchins in the bed was arguably more challenging, and likely less frequent than in the laboratory. Murrain (1999) concludes that that bioturbation by fish, including the stone scorpionfish, *Scorpaena mystes*, is an important mechanism for rhodolith movement in Californian rhodolith beds. The present study did not examine the effects on rhodolith movement and RSL of two fish species frequently encountered in the bed, the winter flounder, *Pseudopleuronectes americanus*, and the winter skate, *Leucoraja ocellata*. Both fish lie on rhodoliths and initiate displacement with quick body undulations that often produce clouds of sediments uplifted from the bed. They also frequently dig in sedimentary bottoms (Grothues et al. 2012). An unknown proportion of the variation in RSL was therefore attributable to bioturbation by both fish and perhaps also by other fish species that spawn their eggs within hollow rhodoliths (Gagnon et al. 2012).

### **Future research directions**

Factors and processes that regulate the structure, function, and stability of rhodolith beds are far less understood than those in long-studied coral reef, seagrass, and kelp bed (forest) systems (Foster 2001, Kaldy & Lee 2007, Montaggioni & Braithwaite 2009, Filbee-Dexter & Scheibling 2014). As pointed out over 15 years ago (Foster 2001) and reiterated

recently (Riosmena-Rodriguez et al. 2017), the rhodolith research community needs to move from short-term, descriptive studies and qualitative correlations, to long-term field studies of factors affecting rhodoliths within and at the distributional limits of beds to gain a better understanding of the causes of bed distribution and dynamics. The present study, which combines experimental testing of bioturbators' effectiveness with short (a few weeks) and longer (a few months) surveys of abiotic and biotic factors potentially affecting rhodolith sediment load and movement at the upper and lower limits of a major rhodolith bed in Newfoundland, is an important step in this direction. In addition to providing clear answers to three main hypotheses about drivers of rhodolith bed stability (see end of the introduction and discussion above), this approach enabled highlighting the key role of rhodolith cryptofauna and macrofauna in preventing accumulation of sediments on rhodoliths, and the different scales (within and outside rhodoliths) at which these bioturbators operate. This is an important aspect of rhodolith bed ecology that had not been demonstrated yet.

Interestingly, ~38% of the spatial and temporal variation in RSL from June to December was explained by factors other than water flow. Multiyear monitoring to capture longer-term variability in water flow, including frequency and intensity of wave storms, as well as studies of the effects of press and pulse disturbances (Tompkins & Steller 2016), are needed to assess resistance and resilience of rhodolith beds to natural and anthropogenic stressors. More detailed studies in controlled environments are also required to determine threshold hydrodynamic forces triggering rhodolith movement and abrasion (Millar and Gagnon, unpublished data). Feeding relationships among rhodolith fauna and flora and their likely connections with phytoplankton and zooplankton are poorly understood and

also deserve greater attention (Hinojosa-Arango & Riosmena-Rodríguez 2004, Grall et al. 2006). Rhodolith beds abound in temperate and sub-arctic Newfoundland and Labrador (Gagnon et al. 2012, Adey et al. 2015) and hold great promise for providing additional answers to key questions in rhodolith bed ecology.

## **CHAPTER III**

### **SUMMARY**

### 3.1. Overall objective of the study

Rhodolith beds are widely distributed marine ecosystems that support a diversity of fauna and flora. Yet, factors and processes that determine the location and extent of beds are poorly understood. The main factors thought to limit the shallow portion of beds are destruction of rhodoliths by high wave action and displacement and subsequent erosion or destruction on bedrock substrate, whereas the deeper portion of beds is presumably limited by light attenuation and sedimentation. If these hypotheses hold true, rhodoliths need to displace enough to limit sedimentation and maintain healthy tissue, but over-displacement leads to abrasion of the live surface or fragmentation. Movement is thought to occur via hydrodynamic forcing (waves and tidal currents) or bioturbation, but the relative role of each and their interaction is poorly understood, with very few studies examining these factors to date. Rhodolith beds organized around the primary productivity of the rhodolith-forming red coralline alga *Lithothamnion glaciale* abound along the coast of Newfoundland. Yet, very little is known about mechanisms of persistence of these beds despite the first report of occurrence of beds in this region over 50 years ago.

The present study tested the relative importance of the hydrodynamic environment and bioturbation in regulating rhodolith sediment load in a large rhodolith bed in southeastern Newfoundland. Specifically, (1) changes in rhodolith sediment load was tracked and modeled over seven months as a function of water flow, sedimentation, and the abundance of dominant rhodolith cryptofauna and macrofauna near the upper and lower margins of the bed; (2) movement of rhodoliths and water flow were measured over three weeks in the centre of the bed, as well as near its upper and lower margins; and (3) the ability of common sea stars [*Asterias rubens*] and green sea urchins [*Strongylocentrotus*

*droebachiensis*] to move rhodoliths was tested in a laboratory mesocosm experiment. The two surveys took place in a rhodolith bed along the coast of St. Philip's, Newfoundland. The laboratory mesocosm experiment was carried out at the Oceans Sciences Centre of Memorial University of Newfoundland with rhodoliths (*L. glaciale*) collected from the bed in St. Philip's.

### **3.2. Importance of the hydrodynamic environment and bioturbation**

Chapter II characterized and parsed spatial and temporal variation in rhodolith sediment load and movement among presumably important abiotic and biotic factors. Specifically, (1) one survey [Field survey 1] monitored sediment load of rhodoliths in the bed as well as water motion and the abundance of four common macrofaunal or cryptofaunal species [*Strongylocentrotus droebachiensis*, *Asterias rubens*, *Tonicella marmorea*, and *Ophiopholus aculeata*] at the upper [12 m depth] and lower [20 m] boundaries of the bed over 7 mo [May to December, 2014]; (2) one survey [Field survey 2] placed marked rhodoliths in permanent frames in the bed and measured displacement for 5 d at three time points during a period when wave activity, and hence the ability to displace rhodoliths, typically intensifies in Newfoundland [13-18 November, 27 November-2 December, and 2-7 December, 2014] and at the upper, middle, and lower boundaries of this bed to capture differences throughout this bed (12, 16, and 20 m); and (3) a mesocosm experiment in floating baskets measured rhodolith displacement every 30 min for 4 h in treatments containing combinations of two common macrofaunal species found within the rhodolith bed – either the presence of one urchin and one sea star, two urchins, two sea stars, or no urchins and no sea stars.

Field survey 1 showed that the biomasses of juvenile common sea stars (*A. rubens*) and brittle stars (*O. aculeata*) and the interaction between month and depth affected rhodolith sediment load. Rhodolith sediment load was inversely related to the biomasses of cryptic *A. rubens* and *O. aculeata*. Sediment at the shallow station was 42% greater than at the deep, and 167% greater in the month with the highest loading (August) compared to the lowest (December). Hydrodynamic forces during this survey did not correlate with sediment loading, and rarely surpassed observed thresholds for rhodolith displacement in Californian rhodolith beds.

Field survey 2 showed that marked rhodolith displacement was highest at the shallow depth and the mid-November time point compared to both the late-November or early-December points. Though recorded water velocity was similar between depths surveyed, movement was 160% greater at the shallow depth (12 m) compared to the deeper depths (16 and 20 m), which were found to not differ from each other. Though water motion was higher in the later time points, displacement at the first time point (13-18 November) was 320% greater than at the other two time points (27 November-2 December, and 2-7 December), which did not differ from each other.

Mesocosm experiment showed that the green sea urchin (*S. droebachiensis*), and not the common sea star (*A. rubens*), is an effective bioturbator of rhodoliths. Displacement in the two-urchin treatment was 77% greater than in the one-urchin-and-one-sea-star treatment, while displacement with two sea stars did not differ from the procedural control (no urchins or sea stars).

### **3.3. Importance of the study**

By downplaying the importance of hydrodynamic forcing as a mechanism regulating rhodolith sediment load in the bed surveyed, while elevating that of bioturbation, the present study clarifies and fuels the debate on factors and processes that regulate the structure, function, and stability of rhodolith beds. Chapter II demonstrated that biotic factors, namely the biomass of daisy brittle stars (*O. aculeata*) and common sea stars (*A. rubens*), along with month and depth are key to limiting sediment load on rhodoliths in southeastern Newfoundland. Rhodolith movement in the field was shown to be highest at the shallow portion of the bed and thrice higher in mid- than late November, yet water speeds were higher at the latter time point. Large (4.5-5.5 cm in test diameter) green sea urchins (*S. droebachiensis*) but not large (10-15 cm in body diameter) common sea stars (*A. rubens*), were effective bioturbators of rhodoliths in laboratory experiments. The present study provides the first quantitative demonstration of differences in the ability of presumed bioturbators to move rhodoliths, while exploring quantitative relationships between hydrodynamic forces and the abundance of bioturbators in Newfoundland rhodolith bed systems. In addition to opening new lines of questioning regarding how these key factors may change on temporal and spatial scales, it points to the importance of both considering multiple factors *in situ* as well as isolating individual factors in a laboratory setting.

### **3.4. Future directions**

The present study provides a framework for further research into the environmental and living components that maintain rhodolith beds. Future studies should focus on resolving the mechanistic processes by which animals may displace both surface sediment

and rhodoliths. This study was largely carried out under natural conditions and so testing how brittle stars (*O. aculeata*) and small sea stars (*A. rubens*) remove sediment, as well as potential predatory interactions under controlled laboratory conditions will give a greater understanding of their role in limiting sediment loading on rhodoliths. Feeding relationships among rhodolith fauna and flora and their likely connections with phytoplankton and zooplankton are poorly understood and also deserve greater attention. Additional factors such as water temperature, seasonality, and presence of predators should also be evaluated as they may be driving forces for these cryptic species. Water speed measured in this study gave a good indication of conditions directly above the surface of the bed, but using technology able to distinguish between oscillatory and unidirectional flows would help understand the non-significance of water flow speeds in this study, as rhodoliths are displaced easier under oscillatory movement. Other factors outside the scope of this study, such as densities of demersal fishes or different shapes of rhodoliths, could help explain trends in sediment loading. Rhodolith research needs to move from short-term, descriptive studies and qualitative correlations, to long-term field studies of factors affecting rhodoliths within and at the distributional limits of beds to gain a better understanding of the causes of bed distribution and dynamics, as this study has done. Repeating surveys on an annual basis within the same system will expand our understanding of how these factors may shift between years. Similar hypotheses should also be tested in other rhodolith beds around the world to test the generality of the results and conclusions. As rhodoliths are made of calcium carbonate, they are at risk of dissolution under the more acidic ocean conditions currently being observed and those predicted for the future due to climate change. Long-term monitoring of potentially

vulnerable rhodolith ecosystems is needed, as predictive capacity of their resilience under changing ocean conditions is hampered by limited baseline knowledge.

## LITERATURE CITED

- Adey WH (1966) Distribution of saxicolous crustose corallines in the northwestern North Atlantic. *J Phycol* 2:49–54
- Adey WH, Adey PJ (1973) Studies on the biosystematics and ecology of the epilithic crustose Corallinaceae of the British Isles. *Br Phycol J* 8:343–407
- Adey WH, Chamberlain YM, Irvine LM (2005) An SEM-based analysis of the morphology, anatomy, and reproduction of *Lithothamnion tophiforme* (esper) Unger (corallinales, Rhodophyta), with a comparative study of associated North Atlantic Arctic/Subarctic Melobesioideae. *J Phycol* 41:1010–1024
- Adey W, Halfar J, Humphreys A, Suskiewicz T, Bélanger D, Gagnon P, Fox M (2015) Subarctic rhodolith beds promote longevity of crustose coralline algal buildups and their climate archiving potential. *PALAIOS* 30:281–293
- Adey WH, Hayek L-AC (2011) Elucidating marine biogeography with macrophytes: Quantitative analysis of the North Atlantic supports the thermogeographic model and demonstrates a distinct subarctic region in the northwestern Atlantic. *Northeast Nat* 18:1–128
- Amado-Filho GM, Moura RL, Bastos AC, Salgado LT, Sumida PY, Guth AZ, Francini-Filho RB, Pereira-Filho GH, Abrantes DP, Brasileiro PS, Bahia RG, Leal RN, Kaufman L, Kleypas JA, Farina M, Thompson FL (2012) Rhodolith beds are major CaCO<sub>3</sub> bio-factories in the tropical south west Atlantic. *PLoS ONE* 7:e35171
- Amado-Filho GM, Pereira-Filho GH (2012) Rhodolith beds in Brazil: a new potential habitat for marine bioprospection. *Rev Bras Farmacogn* 22:782–788
- Amado-Filho GM, Pereira-Filho GH, Bahia RG, Abrantes DP, Veras PC, Matheus Z (2012) Occurrence and distribution of rhodolith beds on the Fernando de Noronha Archipelago of Brazil. *Aquat Bot* 101:41–45
- Ballantine DL, Bowden-Kerby A, Aponte NE (2000) *Cruoriella* rhodoliths from shallow-water back reef environments in La Parguera, Puerto Rico (Caribbean Sea). *Coral Reefs* 19:75–81
- Balsinha MJ, Santos AI, Alves AMC, Oliveira ATC (2009) Textural composition of sediments from Minho and Douro Estuaries (Portugal) and its relation with hydrodynamics. *J Coast Res Suppl Spec Issue SI*:1330–1334
- Basso D (1998) Deep rhodolith distribution in the Pontian Islands, Italy: a model for the paleoecology of a temperate sea. *Palaeogeogr Palaeoclimatol Palaeoecol* 137:173–187

- Basso D, Nalin R, Nelson CS (2009) Shallow-water *Sporolithon* rhodoliths from North Island (New Zealand). *PALAIOS* 24:92–103
- Blain C, Gagnon P (2013) Interactions between thermal and wave environments mediate intracellular acidity (H<sub>2</sub>SO<sub>4</sub>), growth, and mortality in the annual brown seaweed *Desmarestia viridis*. *J Exp Mar Biol Ecol* 440:176–184
- Boer W (2007) Seagrass–sediment interactions, positive feedbacks and critical thresholds for occurrence: a review. *Hydrobiologia* 591:5–24
- Bohm L, Schramm W, Rabsch U (1978) Ecological and physiological aspects of some coralline algae from the western Baltic. Calcium uptake and skeleton formation in *Phymatolithon calcareum*. *Kiel Meeresforsch* 4:282–8
- Bosence DWJ (1983a) The Occurrence and Ecology of Recent Rhodoliths — A Review. In: Peryt DTM (ed) Coated Grains. Springer Berlin Heidelberg, p 225–242
- Bosence DWJ (1983b) The occurrence and ecology of recent rhodoliths - a review. In: Peryt TM (ed) Coated grains. Springer-Verlag, Berlin, p 225–242
- Bosence D, Wilson J (2003) Maërl growth, carbonate production rates and accumulation rates in the ne atlantic. *Aquat Conserv Mar Freshw Ecosyst* 13:S21–S31
- Brodie G, Porter S, Robertson A (1993) Climate and weather of Newfoundland and Labrador. In: Workshop on the Climate and Weather of Newfoundland and Labrador. Creative, St. John's, Nfld., p 152
- Burnham KP, Anderson DR (2004) Multimodel inference: understanding AIC and BIC in model selection. *Sociol Methods Res* 33:261–304
- Cabaço S, Santos R (2007) Effects of burial and erosion on the seagrass *Zostera noltii*. *J Exp Mar Biol Ecol* 340:204–212
- Chen M, Ding S, Liu L, Xu D, Gong M, Tang H, Zhang C (2016) Kinetics of phosphorus release from sediments and its relationship with iron speciation influenced by the mussel (*Corbicula fluminea*) bioturbation. *Sci Total Environ* 542:833–840
- Dahlgren CP, Posey MH, Hulbert AW (1999) The effects of bioturbation on the infaunal community adjacent to an offshore hardbottom reef. *Bull Mar Sci* 64:21–34
- Dearborn J, Edwards K, Fratt D (1981) Feeding biology of sea stars and brittle stars along the Antarctic Peninsula. *Antarct J U S* 16:136–137
- Dethier MN, Steneck RS (2001) Growth and persistence of diverse intertidal crusts: survival of the slow in a fast-paced world. *Mar Ecol Prog Ser* 223:89–100

- Drolet D, Himmelman JH, Rochette R (2004a) Use of refuges by the ophiuroid *Ophiopholis aculeata*: contrasting effects of substratum complexity on predation risk from two predators. *Mar Ecol Prog Ser* 284:173–183
- Drolet D, Himmelman JH, Rochette R (2004b) Effect of light and substratum complexity on microhabitat selection and activity of the ophiuroid *Ophiopholis aculeata*. *J Exp Mar Biol Ecol* 313:139–154
- Dyer KR (2000) Intertidal mudflats: properties and processes. Pergamon, Southampton, U.K.
- Eberly L (2007) Multiple linear regression. In: Ambrosius W (ed) Topics in biostatistics. Humana Press, p 165–187
- Eckman JE, Andres MS, Marinelli RL, Bowlin E, Reid RP, Aspden RJ, Paterson DM (2008) Wave and sediment dynamics along a shallow subtidal sandy beach inhabited by modern stromatolites. *Geobiology* 6:21–32
- Ferrier GA, Carpenter RC (2009) Subtidal benthic heterogeneity: Flow environment modification and impacts on marine algal community structure and morphology. *Biol Bull* 217:115–129
- Filbee-Dexter K, Scheibling R (2014) Sea urchin barrens as alternative stable states of collapsed kelp ecosystems. *Mar Ecol Prog Ser* 495:1–25
- Foster MS (2001) Rhodoliths: between rocks and soft places. *J Phycol* 37:659–667
- Fox J, Weisberg S (2011) An R companion to applied regression, 2<sup>nd</sup> ed. Sage, Thousand Oaks
- Freiwald A (1995) Sedimentological and biological aspects in the formation of branched rhodoliths in northern Norway. *Beitraege Zur Palaeontol* 20:7–19
- Freiwald A, Henrich R (1994) Reefal coralline algal build-ups within the Arctic Circle: morphology and sedimentary dynamics under extreme environmental seasonality. *Sedimentology* 41:963–984
- Frey DL, Gagnon P (2016) Spatial dynamics of the green sea urchin *Strongylocentrotus droebachiensis* in food-depleted habitats. *Mar Ecol Prog Ser* 552:223–240
- Gagnon P, Matheson K, Stapleton M (2012) Variation in rhodolith morphology and biogenic potential of newly discovered rhodolith beds in Newfoundland and Labrador (Canada). *Bot Mar* 55:85–99
- Gaylord B (1999) Detailing agents of physical disturbance: wave-induced velocities and accelerations on a rocky shore. *J Exp Mar Biol Ecol* 239:85–124

- Gaymer CF, Dutil C, Himmelman JH (2004) Prey selection and predatory impact of four major sea stars on a soft bottom subtidal community. *J Exp Mar Biol Ecol* 313:353–374
- Gingold R, Mundo-Ocampo M, Holovachov O, Rocha-Olivares A (2010) The role of habitat heterogeneity in structuring the community of intertidal free-living marine nematodes. *Mar Biol* 157:1741–1753
- Graham DJ, Midgley NG (2000) Graphical representation of particle shape using triangular diagrams: an Excel spreadsheet method. *Earth Surf Process Landf* 25:1473–1477
- Grall J, Hall-Spencer JM (2003) Problems facing maerl conservation in Brittany. *Aquat Conserv Mar Freshw Ecosyst* 13:S55–S64
- Grall J, Le Loc’h F, Guyonnet B, Riera P (2006) Community structure and food web based on stable isotopes ( $\delta^{15}\text{N}$  and  $\delta^{13}\text{C}$ ) analysis of a North Eastern Atlantic maerl bed. *J Exp Mar Biol Ecol* 338:1–15
- Grothues TM, Able KW, Pravatiner JH (2012) Winter flounder (*Pseudopleuronectes americanus* Walbaum) burial in estuaries: acoustic telemetry triumph and tribulation. *J Exp Mar Biol Ecol* 438:125–136
- Gurney WSC, Lawton JH (1996) The population dynamics of ecosystem engineers. *Oikos* 76:273–283
- Hall SJ (1994) Physical disturbance and marine benthic communities: life in unconsolidated sediments. *Oceanogr Mar Biol Annu Rev* 32:179–239
- Hall-Spencer JM, Grall J, Moore PG, Atkinson RJA (2003) Bivalve fishing and maerl-bed conservation in France and the UK: retrospect and prospect. *Aquat Conserv Mar Freshw Ecosyst* 13:S33–S41
- Hall-Spencer J, White N, Gillespie E, Gillham K, Foggo A (2006) Impact of fish farms on maerl beds in strongly tidal areas. *Mar Ecol Prog Ser* 326:1–9
- Himmelman JH, Dutil C (1991) Distribution population structure and feeding of subtidal seastars in the northern Gulf of St. Lawrence. *Mar Ecol Prog Ser* 76:61–72
- Hinchey EK, Schaffner LC, Hoar CC, Vogt BW, Batte LP (2006) Responses of estuarine benthic invertebrates to sediment burial: the importance of mobility and adaptation. *Hydrobiologia* 556:85–98
- Hinojosa-Arango G, Riosmena-Rodríguez R (2004) Influence of rhodolith-forming species and growth-form on associated fauna of rhodolith beds in the central-west Gulf of California, México. *Mar Ecol* 25:109–127

- IPCC (2014) Climate change 2013: the physical science basis. Working group I contribution to the fifth assessment report of the intergovernmental panel on climate change (Stocker, T.F., D Qin, G-K Plattner, SK Tignor, J Allen, AN Boschung, Y Xia, V Bex, and PM Midgley, Eds.). Cambridge University Press, Cambridge
- James DW (2000) Diet, movement, and covering behavior of the sea urchin *Toxopneustes roseus* in rhodolith beds in the Gulf of California, México. *Mar Biol* 137:913–923
- Julien PY (2010) Erosion and sedimentation, 2<sup>nd</sup> ed. Cambridge University Press, Cambridge
- Kaldy JE, Lee K-S (2007) Factors controlling *Zostera marina* L. growth in the eastern and western Pacific Ocean: comparisons between Korea and Oregon, USA. *Aquat Bot* 87:116–126
- Kamenos N (2004) Small-scale distribution of juvenile gadoids in shallow inshore waters; what role does maerl play? *ICES J Mar Sci* 61:422–429
- Kamenos NA, Moore PG, Hall-Spencer JM (2004) Maerl grounds provide both refuge and high growth potential for juvenile queen scallops (*Aequipecten opercularis* L.). *J Exp Mar Biol Ecol* 313:241–254
- Kangeri AK wa, Jansen JM, Joppe DJ, Dankers NMJA (2016) *In situ* investigation of the effects of current velocity on sedimentary mussel bed stability. *J Exp Mar Biol Ecol* 485:65–72
- Kemppainen P, Nes S van, Ceder C, Johannesson K (2005) Refuge function of marine algae complicates selection in an intertidal snail. *Oecologia* 143:402–411
- Klamkin MS (1971) Elementary approximations to the area of n-dimensional ellipsoids. *Am Math Mon* 78:280–283
- Kraufvelin P, Lindholm A, Pedersen MF, Kirkerud LA, Bonsdorff E (2010) Biomass, diversity and production of rocky shore macroalgae at two nutrient enrichment and wave action levels. *Mar Biol* 157:29–47
- Kristensen E, Penha-Lopes G, Delefosse M, Valdemarsen T, Quintana C, Banta G (2012) What is bioturbation? The need for a precise definition for fauna in aquatic sciences. *Mar Ecol Prog Ser* 446:285–302
- Lauzon-Guay J-S, Scheibling RE (2007) Seasonal variation in movement, aggregation and destructive grazing of the green sea urchin (*Strongylocentrotus droebachiensis*) in relation to wave action and sea temperature. *Mar Biol* 151:2109

- Li L, Wang XH, Andutta F, Williams D (2014) Effects of mangroves and tidal flats on suspended-sediment dynamics: Observational and numerical study of Darwin Harbour, Australia. *J Geophys Res Oceans* 119:5854–5873
- Littler MM, Littler DS, Taylor PR (1995) Selective herbivore increases biomass of its prey: A chiton-coralline reef-building association. *Ecology* 76:1666–1681
- Lowe RJ, Falter JL, Bandet MD, Pawlak G, Atkinson MJ, Monismith SG, Koseff JR (2005) Spectral wave dissipation over a barrier reef. *J Geophys Res Oceans* 110:C04001
- Marrack EC (1999) The relationship between water motion and living rhodolith beds in the southwestern Gulf of California, Mexico. *PALAIOS* 14:159–171
- Miller LP, O’Neil MJ, Donnell, Mach KJ (2007) Dislodged but not dead: survivorship of a high intertidal snail following wave dislodgement. *J Mar Biol Assoc U K*
- Montaggioni LF, Braithwaite CJR (2009) Quaternary coral reef systems: history, development processes and controlling factors (H Chamley, Ed.), 1<sup>st</sup> ed. Elsevier, Amsterdam
- Munk JE (1992) Reproduction and growth of green urchins *Strongylocentrotus droebachiensis* (Mueller) near Kodiak, Alaska. *J Shellfish Res* 11:245–254
- Nelson WA (2009) Calcified macroalgae - critical to coastal ecosystems and vulnerable to change: a review. *Mar Freshw Res* 60:787
- Nichols D, Barker MF (1984) Growth of juvenile *Asterias rubens* L. (Echinodermata : Asteroidea) on an intertidal reef in southwestern Britain. *J Exp Mar Biol Ecol* 78:157–165
- Noisette F, Duong G, Six C, Davoult D, Martin S, Hurd C (2013) Effects of elevated pCO<sub>2</sub> on the metabolism of a temperate rhodolith *Lithothamnion corallioides* grown under different temperatures. *J Phycol* 49:746–757
- Piller WE, Rasser M (1996) Rhodolith formation induced by reef erosion in the Red Sea, Egypt. *Coral Reefs* 15:191–198
- Pinet PR (2000) Essential invitation to oceanography, 2<sup>nd</sup> ed. Jones and Bartlett Publishers, Boston
- Prager EJ, Ginsburg RN (1989) Carbonate nodule growth on Florida’s outer shelf and its implications for fossil interpretations. *PALAIOS* 4:310–317
- Quinn GP, Keough MJ (2002) Experimental design and data analysis for biologists. Cambridge University Press, Cambridge

- R Core Team (2014) R: a language and environment for statistical computing. R Foundation for Statistical Computing, Vienna
- Riosmena-Rodríguez R, López-Calderón JM, Mariano-Meléndez E, Sánchez-Rodríguez A, Fernández-García C (2012) Size and distribution of rhodolith beds in the Loreto Marine Park: their role in coastal processes. *J Coast Res* 279:255–260
- Riosmena-Rodríguez R, Nelson W, Aguirre J (Eds) (2017) Rhodolith/maërl beds: a global perspective. Springer International Publishing, Switzerland
- Riul P, Targino CH, Farias JDN, Visscher PT, Horta PA (2008) Decrease in *Lithothamnion* sp. (Rhodophyta) primary production due to the deposition of a thin sediment layer. *J Mar Biol Assoc UK* 88:17–19
- Ryan DA, Brooke BP, Collins LB, Kendrick GA, Baxter KJ, Bickers AN, Siwabessy PJW, Pattiaratchi CB (2007) The influence of geomorphology and sedimentary processes on shallow-water benthic habitat distribution: Esperance Bay, Western Australia. *Estuar Coast Shelf Sci* 72:379–386
- Scheffer M, Portielje R, Zambrano L (2003) Fish facilitate wave resuspension of sediment. *Limnol Oceanogr* 48:1920–1926
- Scheibling R, Hatcher B (2007) Ecology of *Strongylocentrotus droebachiensis*. In: Lawrence J (ed) *Edible sea urchins: biology and ecology*. Elsevier, Amsterdam, p 353–392
- Scheibling RE, Metaxas A (2008) Abundance, spatial distribution, and size structure of the sea star *Protoreaster nodosus* in Palau, with notes on feeding and reproduction. *Bull Mar Sci* 82:221–235
- Schneider CA, Rasband WS, Eliceiri KW (2012) NIH Image to ImageJ: 25 years of image analysis. *Nat Methods* 9:671–675
- Sebens KP (1986) Spatial Relationships among Encrusting Marine Organisms in the New England Subtidal Zone. *Ecol Monogr* 56:73–96
- Sibaja-Cordero JA, Troncoso JS, Benavides-Varela C, Cortés J (2012) Distribution of shallow water soft and hard bottom seabeds in the Isla del Coco National Park, Pacific Costa Rica. *Rev Biol Trop* 60:53–66
- Singer JD, Willett JB (2003) *Applied longitudinal data analysis: modeling change and event occurrence*. Oxford University Press, Oxford
- Smith NP (1994) Long-term Gulf-to-Atlantic transport through tidal channels in the Florida Keys. *Bull Mar Sci* 54:602–609

- Snedecor GW, Cochran WG (1994) *Statistical Methods*, 8<sup>th</sup> ed (DH Jones, Ed.). Iowa State University Press, Ames
- Sneed ED, Folk RL (1958) Pebbles in the lower Colorado River, Texas a study in particle morphogenesis. *J Geol* 66:114–150
- Sokal RR, Rohlf FJ (2012) *Biometry: the principles and practice of statistics in biological research*. W. H. Freeman and Co., New York
- Steller DL, Foster MS (1995) Environmental factors influencing distribution and morphology of rhodoliths in Bahía Concepción, B.C.S., México. *J Exp Mar Biol Ecol* 194:201–212
- Steller DL, Foster MS, Riosmena-Rodriguez R (2009) Living rhodolith bed ecosystems in the Gulf of California. In: Johnson JM, Ledesma-Vázquez J (eds) *Atlas of coastal ecosystems in the Gulf of California: past and present*. University of Arizona Press, Tucson, p 72–82
- Steller DL, Hernández-Ayón JM, Riosmena-Rodriguez R, Cabello-Pasini A (2007) Effect of temperature on photosynthesis, growth and calcification rates of the free-living coralline alga *Lithophyllum margaritae*. *Cienc Mar* 33:441–456
- Steneck RS (1986) The ecology of coralline algal crusts: Convergent patterns and adaptative strategies. *Annu Rev Ecol Syst* 17:273–303
- Storlazzi CD, Field ME, Bothner MH (2011) The use (and misuse) of sediment traps in coral reef environments: theory, observations, and suggested protocols. *Coral Reefs* 30:23–38
- Stotz WB, Aburto J, Caillaux LM, González SA (2016) Vertical distribution of rocky subtidal assemblages along the exposed coast of north-central Chile. *J Sea Res* 107:34–47
- St-Pierre A, Gagnon P (2015) Effects of temperature, body size, and starvation on feeding in a major echinoderm predator. *Mar Biol* 162:1125–1135
- Tecchio S, Coll M, Christensen V, Company JB, Ramírez-Llodra E, Sardà F (2013) Food web structure and vulnerability of a deep-sea ecosystem in the NW Mediterranean Sea. *Deep Sea Res Part Oceanogr Res Pap* 75:1–15
- Teichert S (2014) Hollow rhodoliths increase Svalbard's shelf biodiversity. *Sci Rep* 4:6972
- Thomsen MS, McGlathery K (2006) Effects of accumulations of sediments and drift algae on recruitment of sessile organisms associated with oyster reefs. *J Exp Mar Biol Ecol* 328:22–34

- Thomson RE, Emery WJ (2014) Data analysis methods in physical oceanography, 3<sup>rd</sup> ed. Elsevier, Amsterdam
- Tompkins PA, Steller DL (2016) Living carbonate habitats in temperate California (USA) waters: distribution, growth, and disturbance of Santa Catalina Island rhodoliths. *Mar Ecol Prog Ser* 560:135–145
- Tsuji Y (1993a) Tide Influenced High-Energy Environments and Rhodolith-Associated Carbonate Deposition on the Outer Shelf and Slope Off the Miyako Islands, Southern Ryukyu-Island Arc, Japan. *Mar Geol* 113:255–271
- Tsuji Y (1993b) Tide influenced high energy environments and rhodolith-associated carbonate deposition on the outer shelf and slope off the Miyako Islands, southern Ryukyu Island Arc, Japan. *Mar Geol* 113:255–271
- Turra A, Denadai MR (2006) Microhabitat use by two rocky shore gastropods in an intertidal sandy substrate with rocky fragments. *Braz J Biol* 66:351–355
- Twichell DC, Cross VA, Peterson CD (2010) Partitioning of sediment on the shelf offshore of the Columbia River littoral cell. *Mar Geol* 273:11–31
- Venables WN, Ripley BD (2002) Modern applied statistics with S, 4<sup>th</sup> ed. Springer, New York
- W. J. Woelkerling (1988) The coralline red algae: an analysis of the genera and subfamilies of nongeniculate corallinaceae. British Museum of Natural History ; Oxford University Press, London : Oxford ; New York ; Toronto
- White J (1990) The use of sediment traps in high-energy environments. *Mar Geophys Res* 12:145–152
- Wilson S, Blake C, Berges JA, Maggs CA (2004) Environmental tolerances of free-living coralline algae (maerl): implications for European marine conservation. *Biol Conserv* 120:279–289
- Wright LD, Friedrichs CT, Kim SC, Scully ME (2001) Effects of ambient currents and waves on gravity-driven sediment transport on continental shelves. *Mar Geol* 175:25–45
- Xu M, Sakamoto S, Komatsu T (2016) Attachment strength of the subtidal seaweed *Sargassum horneri* (Turner) C. Agardh varies among development stages and depths. *J Appl Phycol* 28:3679–3687
- Žuljević A, Kaleb S, Peña V, Despalatović M, Cvitković I, Clerck OD, Gall LL, Falace A, Vita F, Braga JC, Antolić B (2016) First freshwater coralline alga and the role of local features in a major biome transition. *Sci Rep* 6:19642

## APPENDIX A

### Comparison of water flow between shallow and deep stations

Mean water flow speed for the deep (20 m) station was available for two blocks of 15 min in each of August, September, October, and November, 2014, for a total of eight blocks. The mean flow speed from each time block at the deep station was paired with the mean flow speed at the shallow station from the 15-min block that (1) preceded the moving of the current meter from shallow to deep, hereafter termed “pre-deep” pairing; and (2) followed the moving of the current meter from deep to shallow, hereafter termed “post-deep” pairing. In doing so, less than three hours separated two time blocks in any given pair, limiting differences in hydrodynamic conditions resulting from regime shifts in broad scale phenomena such as tides and wind-generated waves. Pre-deep and post-deep pairings were both investigated instead of simply one or the other to assess the strength of the conclusions about the difference, or lack thereof, in flow speed between stations. Simple linear regression analysis was used to measure the fit between pre-deep and post-deep flow speed pairings. Both analyses were applied to the raw data ( $n=8$  in each analysis). Two (one for each type of pairing) one-tailed t-tests (two-sample assuming equal variances) were also used to determine if flow speed significantly differed between stations ( $n=16$  in each analysis).

Simple linear regression analysis indicated that flow speeds at the two stations were unrelated in both the pre- and post-deep comparisons (Table A.1). Moreover, mean flow speed in the pre-deep comparison did not differ significantly between the shallow ( $0.036\pm 0.011$  m s<sup>-1</sup>) and deep ( $0.022\pm 0.003$  m s<sup>-1</sup>) stations ( $t_{0.05(1),14}=1.32$ ,  $p=0.270$ ). These results alone suggest that the hydrodynamic environment did not differ between

**Table A.1.** Results of simple linear regression analyses (applied to raw data) examining relationships between mean water flow speed at the deep (20 m) station and mean water flow speed at the shallow (12 m) station before the moving of the current meter from shallow to deep (pre-deep) and after the moving of the current meter from deep to shallow (post-deep) on eight occasions from August to November, 2014. Models' coefficients are shown with corresponding 95% confidence limits (CL).

<b>Data</b>	<b>Intercept (95% CL)</b>	<b>Slope (95% CL)</b>	<b>r<sup>2</sup></b>	<b>F<sub>(df)</sub></b>	<b><i>p</i></b>
Pre-deep	0.025 (0.014, 0.035)	0.065 (-0.030, 0.170)	0.08	0.458 <sub>(1,6)</sub>	0.52
Post-deep	0.018 (0.002, 0.034)	0.094 (-0.211, 0.399)	0.06	0.568 <sub>(1,6)</sub>	0.48

stations. However, mean flow speed in the post-deep comparison was significantly higher at the shallow ( $0.046 \pm 0.009 \text{ m s}^{-1}$ ) station ( $t_{0.05(1),14}=7.07$ ,  $p=0.019$ ), suggesting greater water turbulence there. Sequential moving of the current meter between stations was consistently initiated around 11:00 am to accommodate other subtidal work at the study site. As is typical for that time of day, wind speed and wave action generally increased over the time window needed to complete the first (shallow to deep) and second (deep to shallow) moving. The higher mean flow speed at the shallow station in the post-deep comparison could reflect higher wave-induced water flows at the shallow station after the second moving. Yet, such higher water flows were likely still small enough not to influence the outcome of the regression analysis (Table A.1). Given (1) the poor fit between mean water flow speeds at the two stations [both pre- and post-deep comparisons]; (2) contradictory conclusions from comparing mean flow velocities [significantly different for the post-deep comparison only]; and (3) relatively small sample size [comparisons based on eight days for which flow data were available for both stations], water flow at both stations was deemed similar.

## APPENDIX B

### Breakdown of number of observations used to model rhodolith sediment load

**Table B.1.** Number of observations for each of the nine variables measured at the shallow (12 m) and deep (20 m) stations in the seven months (June to December, 2014) that rhodolith sediment load was monitored. SFS = significant flow speed; SR = sedimentation rate; DSU = density of adult sea urchins on rhodoliths; DSS = density of adult sea stars on rhodoliths; BBS = biomass of cryptic brittle stars; BRC = biomass of cryptic mottled red chitons; BSU = biomass of cryptic sea urchins; BSS = biomass of cryptic sea stars; RSL = Rhodolith sediment load.

Variable	Station	Month							Total
		Jun	Jul	Aug	Sep	Oct	Nov	Dec	
SFS*	Shallow	-	-	-	292	277	212	239	1020
SR*	Shallow	2	4	4	4	4	4	4	26
	Deep	4	4	4	4	3	4	4	27
DSU	Shallow	21	24	21	24	20	24	29	163
	Deep	26	27	22	24	24	25	22	170
DSS	Shallow	21	24	21	24	20	24	29	163
	Deep	26	27	22	24	24	25	22	170
BBS	Shallow	12	12	12	10	12	9	12	79
	Deep	12	11	9	12	12	12	12	80
BRC	Shallow	12	12	12	10	12	9	12	79
	Deep	12	11	9	12	12	12	12	80
BSU	Shallow	12	12	12	10	12	9	12	79
	Deep	12	11	9	12	12	12	12	80
BSS	Shallow	12	12	12	10	12	9	12	79
	Deep	12	11	9	12	12	12	12	80
RSL	Shallow	12	12	12	10	12	9	12	79
	Deep	12	11	9	12	12	12	12	80

\*Variables eliminated from the best-fitting model presented in the results section

## APPENDIX C

### **Explanatory power of water flow and selection of best-fitting model**

Two stepwise regression analyses, one with backward and one with forward selection of model terms, were used to assess the explanatory power of significant flow speed (SFS) on rhodolith sediment load at the shallow (12 m) site for the period during which SFS data was available (September to December, 2014). The removal of SFS from the full model with all candidate variables yielded a substantially more powerful model, as indicated by a drop of 35 in AIC (Table C.1). The addition of SFS to the most basic model containing month as the only candidate variable yielded a substantially less powerful model, with a rise of 160 in AIC (Table C.1). SFS was also highly non-significant in the backward and forward selection models in which it had been included (Table C.2). Accordingly, SFS was deemed unimportant to rhodolith sediment load and was excluded from further analyses of rhodolith sediment load at both sites throughout the entire survey.

The best-fitting model, as identified with stepwise regression analysis of rhodolith sediment load based on data from both sites (12 and 20 m) throughout the entire survey, included the terms DSU, DSS, BBS, BRC, BSU, BSS, S, M, and the interaction between S and M (model 4 in Table C.3). This model presented a much lower AIC (189, with an  $\Delta$ AIC of 3) than that of the next less powerful model (model 5 in Table C.3 with an AIC of 608 and  $\Delta$ AIC of 422). It was chosen over three models with comparable AICs (models 1 to 3 in Table C.3) because it was the most conservative of these models, presenting the highest number of candidate variables. Interestingly, elimination of

**Table C.1.** Results of stepwise regression analysis of rhodolith sediment load examining the Akaike Information Criterion (AIC) and variation in AIC ( $\Delta$ AIC) from one model to the next, in backward and forward model terms selection modes, based on data collected at the shallow (12 m) site for the period during which significant flow speed data was available (September to December, 2014). SFS = significant flow speed; SR = sedimentation rate; DSU = density of adult sea urchins on rhodoliths; DSS = density of adult sea stars on rhodoliths; BBS = biomass of cryptic brittle stars; BRC = biomass of cryptic mottled red chitons; BSU = biomass of cryptic sea urchins; BSS = biomass of cryptic sea stars; M = sampling month.

<b>Elimination mode</b>	<b>Model</b>	<b>AIC</b>	<b><math>\Delta</math>AIC</b>
Backward	1. <b>SFS</b> +SR+DSU+DSS+BBS+BRC+BSU+BSS+M	96	35
	2. SR+DSU+DSS+BBS+BRC+BSU+BSS+M	61	0
Forward	1. M	176	0
	2. <b>SFS</b> +M	336	160

**Table C.2.** Model terms significance for the least two performant models including significant flow speed presented in Table C.1 (n=1445 [backward] and 1063 [forward]). SFS = significant flow speed; SR = sedimentation rate; DSU = density of adult sea urchins on rhodoliths; DSS = density of adult sea stars on rhodoliths; BBS = biomass of cryptic brittle stars; BRC = biomass of cryptic mottled red chitons; BSU = biomass of cryptic sea urchins; BSS = biomass of cryptic sea stars; M = sampling month.

Elimination mode	Source of variation	<i>df</i>	MS	F-value	<i>p</i>
Backward	<b>SFS</b>	1	0.33	0.16	0.71
	SR	1	0.46	0.22	0.66
	DSU	1	1.13	0.54	0.50
	DSS	1	3.78	1.83	0.25
	BBS	1	0.02	0.01	0.93
	BRC	1	2.40	1.16	0.34
	BSU	1	1.16	0.56	0.50
	BSS	1	5.71	2.76	0.17
	M	3	6.52	3.15	0.15
	Error	4	2.07		
	Total	15			
Forward	<b>SFS</b>	1	0.20	0.10	0.75
	M	3	25.21	12.59	<0.001
	Error	43	2.00		
	Total	47			

**Table C.3.** Results of stepwise regression analysis of rhodolith sediment load examining the Akaike Information Criterion (AIC) and variation in AIC ( $\Delta$ AIC) from one model to the next, in backward model terms selection mode, based on data collected at the shallow (12 m) and deep (20 m) sites for the entire duration of the survey (6 June to 7 December, 2014). SR = sedimentation rate; DSU = density of adult sea urchins on rhodoliths; DSS = density of adult sea stars on rhodoliths; BBS = biomass of cryptic brittle stars; BRC = biomass of cryptic mottled red chitons; BSU = biomass of cryptic sea urchins; BSS = biomass of cryptic sea stars; S = sampling station; M = sampling month.

Model	AIC	$\Delta$ AIC
1. DSU+ BBS+ BSU+BSS+S+M+S*M	186	0
2. DSU+ BBS+ BRC+BSU+BSS+S+M+S*M	187	1
3. DSU+DSS+BBS+ BRC+ BSS+S+M+S*M	188	2
4. DSU+DSS+BBS+ BRC+BSU+BSS+S+M+S*M	189	3
5. SR+DSU+DSS+BBS+ BRC+BSS+S+M+S*M	608	422
6. SR+DSU+DSS+BBS+BRC+BSU+BSS+S+M+S*M	610	424
7. SR+DSU+DSS+BBS+ BSU+BSS+S+M+S*M	612	426

sedimentation rate (SR) dramatically improved model performance, as shown by a change in  $\Delta AIC$  from 422 to 3 in respectively the best- and next less-fitting models (models 4 and 5 in Table C.3). Accordingly, the model that best explained variation in rhodolith sediment load was:

DSU+DSS+BBS+BRC+BSU+BSS+S+M+S\*M

## APPENDIX D

### Outcome of statistical analyses for Figure 2.3

**Table D.1.** Summary of two-way ANOVA (applied to raw data) examining the effect of Depth (12 and 20 m), Month (June to December, 2014), and their interaction on rhodolith sediment load in Field survey 1.

Source of variation	<i>Df</i>	MS	F-value	<i>p</i>
Depth	1	46.985	19.361	<0.001
Month	6	32.574	13.423	<0.001
Depth x Month	6	6.052	2.494	0.025
Error	154	2.427		
Corrected total	167			

**Table D.2.** Summary of two-way ANOVA (applied to raw data) examining the effect of Depth (12 and 20 m), Month (June to December, 2014), and their interaction on sedimentation rate in Field survey 1.

Source of variation	<i>Df</i>	MS	F-value	<i>p</i>
Depth	1	1.647 x 10 <sup>-6</sup>	41.92	<0.001
Month	6	2.800 x 10 <sup>-6</sup>	71.24	<0.001
Depth x Month	6	1.548 x 10 <sup>-7</sup>	3.94	0.004
Error	39	3.931 x 10 <sup>-8</sup>		
Corrected total	52			

## APPENDIX E

### Outcome of statistical analyses for panels A to I in Figure 2.5

**Table E.1.** Summary of two-way ANOVA (applied to raw data) examining the effect of Depth (shallow [12 m] and deep [20 m] stations) and Month (the seven months in which rhodolith sediment load was measured; June to December, 2014) on the density of large green sea urchins (*Strongylocentrotus droebachiensis*) on rhodoliths in Field survey 1 (see section 2.2.2.3 for sampling details).

Source of variation	<i>Df</i>	MS	F-value	<i>P</i>
Depth	1	1.618 x 10 <sup>-4</sup>	26.48	<0.001
Month	6	8.235 x 10 <sup>-6</sup>	1.35	0.236
Depth x Month	6	1.004 x 10 <sup>-5</sup>	1.64	0.135
Error	319	6.112 x 10 <sup>-6</sup>		
Corrected total	332			

**Table E.2.** Summary of two-way ANOVA (applied to raw data) examining the effect of Depth (shallow [12 m] and deep [20 m] stations) and Month (the seven months in which rhodolith sediment load was measured; June to December, 2014) on the density of large common sea stars (*Asterias rubens*) on rhodoliths in Field survey 1 (see section 2.2.2.3 for sampling details).

Source of variation	<i>Df</i>	MS	F-value	<i>P</i>
Depth	1	2.200 x 10 <sup>-6</sup>	4.96	0.027
Month	6	2.854 x 10 <sup>-7</sup>	0.64	0.695
Depth x Month	6	8.195 x 10 <sup>-7</sup>	1.85	0.089
Error	319	4.432 x 10 <sup>-7</sup>		
Corrected total	332			

**Table E.3.** Summary of two-way ANOVA (applied to raw data) examining the effect of Depth (shallow [12 m] and deep [20 m] stations) and Month (the seven months in which rhodolith sediment load was measured; June to December, 2014) on the wet weight of daisy brittle stars (*Ophiopholis aculeata*) within rhodoliths interstices in Field survey 1 (see section 2.2.2.4 for sampling details).

Source of variation	<i>df</i>	MS	F-value	<i>p</i>
Depth	1	92.806	68.90	<0.001
Month	6	4.690	3.48	0.003
Depth x Month	6	2.423	1.80	0.103
Error	145	1.347		
Corrected total	158			

**Table E.4.** Summary of two-way ANOVA (applied to raw data) examining the effect of Depth (shallow [12 m] and deep [20 m] stations) and Month (the seven months in which rhodolith sediment load was measured; June to December, 2014) on the wet weight of mottled red chitons (*Tonicella marmorea*) within rhodoliths interstices in Field survey 1 (see section 2.2.2.4 for sampling details).

Source of variation	<i>df</i>	MS	F-value	<i>p</i>
Depth	1	0.155	11.87	<0.001
Month	6	0.038	2.91	0.010
Depth x Month	6	0.015	1.13	0.346
Error	145	0.013		
Corrected total	158			

**Table E.5.** Summary of two-way ANOVA (applied to raw data) examining the effect of Depth (shallow [12 m] and deep [20 m] stations) and Month (the seven months in which rhodolith sediment load was measured; June to December, 2014) on the wet weight of small green sea urchins (*Strongylocentrotus droebachiensis*) within rhodoliths interstices in Field survey 1 (see section 2.2.2.4 for sampling details).

Source of variation	<i>df</i>	MS	F-value	<i>p</i>
Depth	1	2.349	16.43	<0.001
Month	6	0.352	2.46	0.027
Depth x Month	6	0.076	0.53	0.782
Error	145	0.143		
Corrected total	158			

**Table E.6.** Summary of two-way ANOVA (applied to raw data) examining the effect of Depth (shallow [12 m] and deep [20 m] stations) and Month (the seven months in which rhodolith sediment load was measured; June to December, 2014) on the wet weight of small common sea stars (*Asterias rubens*) within rhodoliths interstices in Field survey 1 (see section 2.2.2.4 for sampling details).

Source of variation	<i>df</i>	MS	F-value	<i>p</i>
Depth	1	0.020	1.38	0.242
Month	6	0.022	1.51	0.179
Depth x Month	6	0.028	1.94	0.079
Error	145	1.347		
Corrected total	158			